



**Small Scale Electricity Production from Low
Temperature Geothermal Resources Using
Organic Rankine Cycle**

Emilía Valdimarsdóttir

Thesis of 60 ECTS credits
**Master of Science (M.Sc.) in Sustainable Energy
Engineering**

January 2017



Small Scale Electricity Production from Low Temperature Geothermal Resources Using Organic Rankine Cycle

by

Emilía Valdimarsdóttir

Thesis of 60 ECTS credits submitted to the School of Science and Engineering
at Reykjavík University in partial fulfillment
of the requirements for the degree of
Master of Science (M.Sc.) in Sustainable Energy Engineering

January 2017

Supervisor:

María Sigríður Guðjónsdóttir,
Assistant Professor, Reykjavík University, Iceland

Jón Matthíasson,
Innovation Center Iceland, Reykjavík, Iceland

Examiner:

Einar Jón Ásbjörnsson,
Assistant Professor, Reykjavik University, Iceland

Copyright
Emilía Valdimarsdóttir
January 2017

Small Scale Electricity Production from Low Temperature Geothermal Resources Using Organic Rankine Cycle

Emilía Valdimarsdóttir

January 2017

Abstract

The most common use of geothermal energy for electricity production is by using the fluid in its vapor state. Low temperature geothermal sources in liquid form are, in many areas in Iceland, used for district heating. Another possible utilization of the low temperature geothermal resource is to generate electricity by the use of binary cycles. Binary cycles are well known throughout the world and the most common cycle is the Organic Rankine Cycle (ORC). The ORC uses a low temperature geothermal resource to heat up a working fluid, that has a lower boiling point than water. The objective of this study was to model an ORC unit in Engineering Equation Solver (EES) in order to produce 100 kW of electricity for a small scale user such as a greenhouse. The motivation for this thesis was an existing ORC unit that was built by XRG Power and the Innovation Center in 2015. That unit produces 1 kW and this model's main focus was to scale that power output up to 100 kW, and find out whether that unit would be a feasible investment for greenhouse owners. A model was made in EES and components of the ORC explained. A working fluid comparison study was performed and the working fluid R1234yf was chosen as the best option based on given assumptions. An economic feasibility study was performed and it was concluded that this 100 kW ORC unit is an investment worth making for greenhouse owners. A case study was performed for an Icelandic greenhouse and, even though the model delivered less than the model's ambition, it was concluded that the unit would be a good investment for that greenhouse. A comparison was made with the XRG unit and different parameters tested. This study provides a basis for continuing research of this subject.

Notkun Organic Rankine Cycle til raforkuframleiðslu úr lághita jarðvökva

Emilía Valdimarsdóttir

janúar 2017

Útdráttur

Raforkuframleiðsa notast yfirleitt við jarðvökva í gufufasa. Á mörgum stöðum á Íslandi er notast við lághita jarðvökva til hitaveitu. Annað mögulegt notagildi er að framleiða rafmagn með notkun tvívökva kerfa. Tvívökvavélar eru þekktar um allan heim og algengasta tvívökva kerfið er Organic Rankine Cycle (ORC). ORC kerfið notar lághita jarðvökva til að hita upp vinnsluvökva sem hefur lægra suðumark. Markmið þessarar ritgerðar var að gera líkan af ORC kerfi í Engineering Equation Solver (EES) sem framleiðir 100 kW af raforku fyrir notendur svo sem gróðurhús. Hvatinn að þessu verkefni var ORC kerfi sem smíðað var af XRG Power og Nýsköpunarmiðstöðinni 2015. Það kerfi framleiðir 1 kW af raforku og átti þetta líkan að skila hundraðföldu afli, eða 100 kW, og komast að því hvort slíkt kerfi yrði ákjósanleg fjárfesting fyrir gróðurhúsabændur. Líkan var gert í EES og hlutar kerfisins útskýrðir nánar. Vinnsluvökvasamanburður var gerður og ákveðið var að vinnsluvökvinn R1234yf yrði ákjósanlegasti kosturinn. Hagkvæmniútreikningar sýndu að 100 kW ORC kerfið yrði góð fjárfestingin fyrir gróðurhúsabændur. Raunverulegt dæmi var tekið fyrir, íslenskt gróðurhús, og þó að líkanið, með skilyrðum, skilaði töluvert minna afli en 100 kW var niðurstaðan sú að fjárfestingin er vel þess virði fyrir gróðurhúsabóndann. Samanburður við XRG kerfið var gerður og er þessi ritgerð grunnur fyrir áframhaldandi rannsóknir á þessum þáttum.

Small Scale Electricity Production from Low Temperature Geothermal Resources Using Organic Rankine Cycle

Emilía Valdimarsdóttir

Thesis of 60 ECTS credits submitted to the School of Science and Engineering
at Reykjavík University in partial fulfillment of
the requirements for the degree of
Master of Science (M.Sc.) in Sustainable Energy Engineering

January 2017

Student:

.....
Emilía Valdimarsdóttir

Supervisor:

.....
María Sigríður Guðjónsdóttir

.....
Jón Matthíasson

Examiner:

.....
Einar Jón Ásbjörnsson

The undersigned hereby grants permission to the Reykjavík University Library to reproduce single copies of this Thesis entitled **Small Scale Electricity Production from Low Temperature Geothermal Resources Using Organic Rankine Cycle** and to lend or sell such copies for private, scholarly or scientific research purposes only.

The author reserves all other publication and other rights in association with the copyright in the Thesis, and except as herein before provided, neither the Thesis nor any substantial portion thereof may be printed or otherwise reproduced in any material form whatsoever without the author's prior written permission.

.....
Date

.....
Emilía Valdimarsdóttir
Master of Science

For my children

Acknowledgements

I would like to thank my supervisor, Dr. María Guðjónsdóttir for her excellent guidance throughout this process as well as Jón Matthíasson, at the Innovation Center Iceland, for applying me with data for comparison and technical assistance.

Special thanks go to Vašek Novotný for programming and thermodynamics assistance.

My gratitude extends to all my friends, who helped and supported me in different ways, especially Birna Sif Kristínardóttir for helpful comments.

Thanks to my daughter, for being patient throughout my years of studying and last, but not least, my girlfriend, Hrafnhildur Skúladóttir, who has helped me in numerous ways and supported me throughout this process.

Contents

Acknowledgements	x
Contents	xi
List of Figures	xiii
List of Tables	xv
List of Abbreviations	xvi
List of Symbols	xvii
1 Introduction	1
2 Background	3
2.1 Geothermal Utilization	3
2.1.1 Geothermal Utilization in Iceland	4
2.1.1.1 Geothermal Utilization in Greenhouses	4
2.2 Small Scale Electricity Generation	6
2.3 Binary Cycles	6
2.3.1 Organic Rankine Cycle	6
2.4 The XRG Unit	7
3 Methods	9
3.1 Geothermal Utilization in Greenhouses in Iceland	9
3.2 Turbine vs. Expander	10
3.3 Modelling	11
3.3.1 Cycle States	12
3.3.2 Individual Components	13
3.3.2.1 Heat Exchangers	14
3.3.2.2 Pump	23
3.3.2.3 Turbine	23
3.4 Comparable Commercial ORC Units	26
3.5 Working Fluids	27
3.6 Economic Feasibility	33
3.6.1 Electricity Prices for Greenhouses in Iceland	34
3.6.2 Cost Benefit Analysis	35
3.6.2.1 Net Present Value	37
3.7 Case Study - Friðheimar	38
3.8 Model Comparison with the XRG Unit	41

4	Results	49
4.1	Base Case	49
4.2	Economic Feasibility Results	50
4.3	Case Study Results	51
4.4	Model Comparison	52
5	Discussion	54
5.1	Base Case	54
5.2	Working Fluid Selection	55
5.3	Economic Feasibility	55
5.4	Case Study	56
5.5	Model Comparison	56
5.6	Assumptions & Future Work	57
5.7	Conclusion	58
	Bibliography	60
A	Code	64

List of Figures

2.1	Iceland's divergent plate boundary (Mira Costa College, 2016).	4
2.2	A map of Iceland showing the location of greenhouses using geothermal resources for heating (Orkustofnun, 2016).	5
2.3	A typical Organic Rankine Cycle including major components needed (Borunda, Jaramillo, Dorantes, and Reyes, 2015).	7
2.4	The XRG unit and the team behind the design and construction. From the left: Sverrir Kári Karlsson, Jón Matthíasson, Þorsteinn Ingi Sigfússon, Mjöll Waldorff and Nils Erik Gíslason (Nýsköpunarmiðstöð Íslands, 2015).	8
3.1	A schematic of different types of expanders (Weiß, 2015)	11
3.2	A schematic of different types of turbines (Weiß, 2015)	11
3.3	A block diagram of an Organic Rankine Cycle	13
3.4	A schematic showing a typical plate heat exchanger (Northern Lights. Solar Solutions, 2016).	14
3.5	A graph showing the temperature and heat transfer correlation in the evaporator	16
3.6	A graph showing the temperature and heat transfer correlation in the condenser	17
3.7	Location of temperatures used in the LMTD calculation for the evaporator . . .	20
3.8	Location of temperatures used in the LMTD calculation for the condenser . . .	21
3.9	Correction factor chart for cross flow heat exchangers. T referring to the hotter fluid's temperatures, t referring to the colder fluid's temperatures and subscripts 1 and 2 representing inlet and outlet. (Bergman, Lavine, Incropera, and DeWitt, 2011).	22
3.10	The cycle including conditions chosen for working fluid comparison	29
3.11	Net Power output of different working fluids	31
3.12	Cycle thermal efficiency of different working fluids	31
3.13	T-s diagrams of Toluene on top, D4 on the left and D5 on the right	32
3.14	T-s diagrams of R134a on the left and R245fa on the right	32
3.15	T-s diagrams of Isopentane on the left and R123 on the right	33
3.16	T-s diagrams of R1234yf on the left and R1234ze(E) on the right	33
3.17	Location of Friðheimar Greenhouse (marked with a star) (Orkustofnun, 2016) .	38
3.18	Location of Friðheimar Greenhouse and the borehole Reykholtshver (marked with a star) (Google Maps, 2016)	39
3.19	A schematic of the model's ORC cycle including temperature and mass flow rate of Friðheimar's geothermal resource	40
3.20	The XRG unit's geothermal fluid's inlet temperature measurements	41
3.21	The XRG unit's geothermal fluid's outlet temperature measurements	42
3.22	The XRG unit's mass flow rate of the hot water measurements	42
3.23	The XRG unit's cooling water temperature inlet measurements	43
3.24	The XRG unit's cooling water temperature outlet measurements	43

3.25	The XRG unit's mass flow rate of the cooling water measurements	44
3.26	The XRG unit's mass flow rate of the working fluid measurements	44
3.27	The XRG unit's scroll expander power output measurements	45
3.28	The XRG unit's scroll expander inlet temperature measurements	45
3.29	The XRG unit's scroll expander outlet temperature measurements	46
3.30	The XRG unit's scroll expander inlet pressure measurements	46
3.31	The XRG unit's scroll expander outlet pressure measurements	47
4.1	A visual representation of the effects of mass flow rate and temperature on net power output	50

List of Tables

3.1	Comparison of greenhouses' geothermal resources utilization. *No data found .	10
3.2	Commercial ORC units' parameters, comparable to the case in this study	26
3.3	Commercial ORC units' parameters, cont.	27
3.4	Physical properties of selected working fluids (Nouman, 2012)	29
3.5	Environmental properties of selected working fluids (Nouman, 2012) (Navea, Young, Xu, Grassian, and Stanier, 2011) *No data found	30
3.6	Safety data of selected working fluids (Nouman, 2012) (Datla and Brasz, 2012)	30
3.7	Electricity sellers price of electricity (Orkusetur, 2016)	34
3.8	Electricity distributors price of distribution (Orkusetur, 2016) (Guðmundsson, 2016)	35
3.9	Parameters from the XRG unit	48
4.1	Modelling results	49
4.2	Heat exchangers design results	50
4.3	Variables summary	51
4.4	Case study NPV variables	51
4.5	Case Study results	52
4.6	Average values from measurements	52
4.7	Comparison between the XRG unit and this studies unit	53

List of Abbreviations

<i>BWR</i>	Back Work Ratio
<i>C</i>	Condenser
<i>CBA</i>	Cost Benefit Analysis
<i>DSH</i>	De-Super-heater
<i>EES</i>	Engineering Equation Solver
<i>EV</i>	Evaporator
<i>GWP</i>	Global Warming Potential
<i>HVACR</i>	Heating, Ventilation, Air Conditioning and Refrigeration
<i>kWh</i>	Kilowatthours
<i>LFL</i>	Lower Flammability Limit
<i>LMTD</i>	Log Mean Temperature Difference
<i>min</i>	Minutes
<i>NPV</i>	Net Present Value
<i>OPD</i>	Ozone Depletion Potential
<i>ORC</i>	Organic Rankine Cycle
<i>O&M</i>	Operations and maintenance
<i>PH</i>	Preheater
<i>PHE</i>	Plate Heat Exchanger
<i>SC</i>	Sub-cooler
<i>SH</i>	Super-heater

List of Symbols

Symbol	Description	Unit
A	Area	m^2
B	Loan Amount	ISK
C	Cash Flow	ISK
F	Correction factor	
h	Enthalpy	kg/kJ
\dot{m}	Mass flow rate	kg/s
n	Number of years	
P	Payment	ISK
P	Pressure	bar
q	Heat flux	kJ
r	Discount rate	%
s	Entropy	kJ/kgK
T	Temperature	$^{\circ}\text{C}$
u	Velocity	m/s
U	Overall heat transfer coefficient	$\text{W/m}^2\text{^{\circ}C}$
\dot{V}	Volumetric flow rate	m^3/s
W	Power	kW
X	Steam quality	%
Δ	Difference	
η	Efficiency	%
ν	Specific volume	m^3/kg

Subscripts

1, 2, 3, 4, 5, 6, 7, 8	State number
<i>avg</i>	Average
<i>boil</i>	Boiler (Evaporator)
<i>c</i>	Colder fluid
<i>car</i>	Carnot
<i>cond</i>	Condenser
<i>h</i>	Hotter fluid
<i>in</i>	Inlet
<i>is</i>	Is-entropic
<i>lm</i>	Log Mean Temperature difference
<i>out</i>	Outlet
<i>pump</i>	Pump
<i>r</i>	Ratio
<i>th</i>	Thermal
<i>turb</i>	Turbine
<i>wf</i>	Working fluid

Chapter 1

Introduction

During the past century, global surface temperatures have been increasing, a phenomenon called the global warming. Global warming is believed to be caused by the accumulation of various gasses in the Earth's atmosphere, however, the main culprit is carbon dioxide. Release of these gasses, usually known as "greenhouse gasses", has increased by 40% since the mid 18th century. As mentioned, the gasses accumulate in the atmosphere, wherein they eventually lead to an increase in global temperatures since they block the reflection of excess solar radiation back to space. Over the past few decades, this fact has triggered an interest in utilizing renewable energy sources, particularly, how these sources can be exploited in an efficient manner, which in turn, could decrease the emission of detrimental greenhouse gasses (Ocko, 2016). Assuming it is not too late, using renewable energy sources can slow down this process since they do not, or at least in small amounts, release greenhouse gasses in the atmosphere. In this study renewable energy sources, geothermal, are used to produce electricity in a small and sustainable manner.

The inspiration for this study came from the Innovation Center Iceland. The idea of modelling an Organic Rankine Cycle that could produce 100 kW of electrical energy was approached by them early in the year 2016. They had, along with XRG Power, built a 1 kW unit and wanted to scale that up and produce more electricity for users with higher electricity needs, such as greenhouses.

This study includes a background of the technology needed as well as an introduction of greenhouses in Iceland and the utilization of geothermal resources. Furthermore it also includes a model of an Organic Rankine Cycle, modelled in Engineering Equation Solver (EES) (F-Chart Software, 2016), individual components analysis, parameters of commercial ORC units and working fluids will be compared and a suitable fluid selected for this model. Economic feasibility calculations were made with regards to the investment made by a greenhouse owner in order to predict whether or not this is a viable investment to make. A case study of a greenhouse, Friðheimar, was made in order to supply an example of how this technology could benefit in realistic conditions. Lastly, a comparison was made with the XRG unit.

Chapter 2

Background

For a deeper understanding of this topic, a background is provided in the following sections. Geothermal energy and small-scale utilization will be explained followed by an introduction into the technology of Organic Rankine Cycles. Geothermal utilization for greenhouses in Iceland will be researched and lastly, the XRG unit, the one this project is based on will be further explained.

2.1 Geothermal Utilization

Geothermal energy is, as the word implies, thermal energy from the ground. At the center of the Earth, the temperatures are estimated to be around 6.650°C . For a geothermal system to be prosperous, it needs a heat source, permeability, and water and in order to utilize the resource surface and subsurface exploration is needed. This exploration involves researching the area underground and the best location is mapped. To reach desired temperatures and pressures this location is drilled into and the fluid is pumped, or flows freely, up the well.

Geothermal fluid can be extracted from the geothermal resource in a wide range of temperatures, usually covering a range from 50 to 350°C . It can be in different forms, liquid, steam or a mixture of both. Temperature plays a determining role in how well the fluid performs in electricity production. High-temperature fluid, in the form of steam, is most suitable for electricity production through steam cycles due to their high energy content and high steam

quality, meaning that the fluid is pure steam. The steam is directly routed through the turbine to produce electricity (DiPippo, 2012).

2.1.1 Geothermal Utilization in Iceland

The Earth gradually cools down towards the surface due to heat transfer via conduction and convection. The temperature increase downwards, in regards to depth, is called a temperature gradient. This gradient is highly diverse in different places around the globe. The location of the land with regards to tectonic plate boundaries plays a major role. In areas, such as Iceland, where the plate boundaries are divergent the gradient is high. Divergent means that the plates are moving in opposite directions, 2 cm/year in Iceland. The temperature gradient in Iceland is close to $300\text{ }^{\circ}\text{C}/\text{km}$ closest to plate boundaries and therefore one does not have to dig very deep to reach high temperatures. This number is ten times higher than the world's average of $30\text{ }^{\circ}\text{C}/\text{km}$. Due to those special conditions Iceland plays a leading role worldwide in geothermal utilization (DiPippo, 2012). Figure 2.1 illustrates how Iceland is located on a divergent plate boundary.

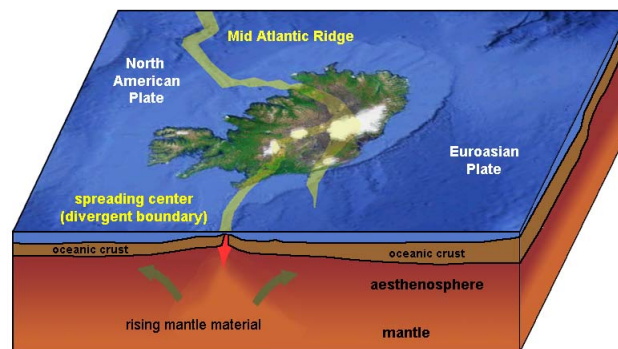


Figure 2.1: Iceland's divergent plate boundary (Mira Costa College, 2016).

2.1.1.1 Geothermal Utilization in Greenhouses

In 2008, the greenhouse in Iceland heated by geothermal fluid covered an area of about 192.000 m^2 , almost half of them are located in the southern part of Iceland and most of them are close to the divergent plate boundaries. Greenhouse owners have been using a

substantial amount of electricity for lighting since the 1970's. Greenhouses in Iceland are dependant on these artificial lights, due to the lack of sunlight in Iceland for nearly half of the year, to produce a variety of vegetables year round including tomatoes, cucumbers, bell peppers, lettuce, berries and mushrooms as well as numerous herbs and even flowers. In the year 2015, greenhouse owners were using over 80 GWh of electricity, equivalent to the use of about 15.000 homes in Iceland. This number has been rapidly increasing, about 4% per year, in the past years and decades and has almost doubled since 2004 (Vilhjálmsson, Baldursson, and Hallgrímsson, 2015). The greenhouses utilize hot, geothermal fluid from nearby boreholes, usually owned by the greenhouse owner, to heat up their facilities due to cold conditions. This water is pumped from the boreholes and transported by pipes to the greenhouses.

In Figure 2.2 a map of Iceland shows the location of greenhouses that currently use geothermal waters from nearby boreholes to heat up their facilities.



Figure 2.2: A map of Iceland showing the location of greenhouses using geothermal resources for heating (Orkustofnun, 2016).

2.2 Small Scale Electricity Generation

Small scale electricity generation, otherwise known as micro-generation is the production of electricity or heat on a very small scale compared to typical power stations. Micro-generators are especially useful in remote areas where connection to the grid is limited or non-existing. It can also benefit small businesses or individuals to lower their carbon footprint and reduce their electricity costs and become sustainable. The majority of micro-generators are environmentally friendly and in most instances emit no carbon into the environment. They use different sources for energy; solar, geothermal, wind or biomass (Microgeneration, 2016).

2.3 Binary Cycles

In low temperature geothermal resources, it is common to use binary cycles to make it possible to produce electricity (Hettiarachci, Golubovic, Wore, and Ikegami, 2006). Different types of binary cycles include dual-pressure cycles, dual-fluid cycles, Kalina cycles and Organic Rankine cycle (DiPippo, 2012). This study uses an Organic Rankine Cycle.

2.3.1 Organic Rankine Cycle

The Organic Rankine Cycle (ORC) has been used since the 1960's to generate electricity from low temperature geothermal fluid (Lund, 2004). The basic concept is that the ORC uses heat from a geothermal fluid to heat up a working fluid. The main components are an evaporator, to heat up and evaporate the working fluid, a turbine that produces mechanical energy that is then transformed in to electricity by a generator. An alternative to a turbine is an expander. The difference between the two will be discussed in section 3.2. After that the vapor is directed to a condenser, to condense the vapor back to liquid and lastly, a pump to get it back to the evaporator. The working fluid is a fluid that has a lower boiling point than the geothermal fluid. It cycles through this process continuously in an isolated loop. The evaporator is a heat exchanger that, in this study, uses the hot geothermal brine to heat

up the working fluid, and the condenser is a heat exchanger as well that cools the working fluid down with the use of cooling water, air or an alliterative fluid (Wei, Lu, Lu, and Gu, 2006). This process is further described in subsection 3.3.1. A schematic of a typical ORC including major components is seen in Figure 2.3.

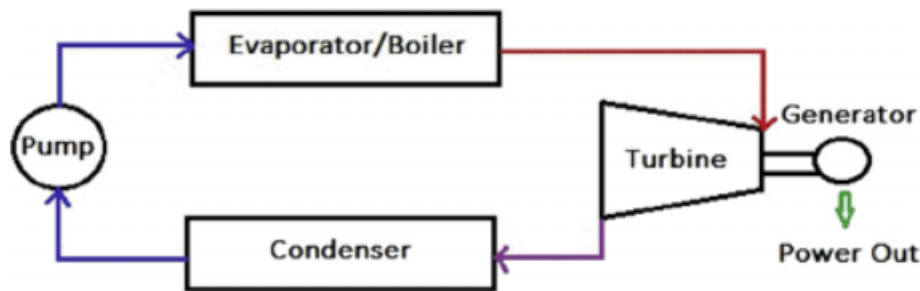


Figure 2.3: A typical Organic Rankine Cycle including major components needed (Borunda, Jaramillo, Dorantes, and Reyes, 2015).

2.4 The XRG Unit

XRG Power is a company which was founded by The Innovation Center Iceland and Hjalti Einarsson's Machine shop in early 2015 with the goal of producing electricity from low heat geothermal resources using micro binary generators. This geothermal fluid would be at a temperature range of 70-135 °C. XRG power aims to produce small, cost efficient personal generators. The motivation behind this project was to make use of otherwise unused resources to produce electricity in an environmentally friendly way. The company made a prototype that could generate 1 kW of electrical energy. This unit can be used by small scale users, especially intended for remote areas where there may be a need to rely on fossil fuels due to lack of access to the local electricity grid. They intend on taking this unit to foreign markets with three main applications; telecommunications for remote areas, cottages and cabins and small boats and vessels. For boats and vessels the access heat from various machinery on board would be used instead of the geothermal resource intended for the other types. In the fall of 2015, they had a working prototype (Waldorff, 2016). Figure 2.4 shows the XRG unit along with the group of people responsible for its design and construction.



Figure 2.4: The XRG unit and the team behind the design and construction. From the left: Sverrir Kári Karlsson, Jón Matthíasson, Þorsteinn Ingi Sigfússon, Mjöll Waldorff and Nils Erik Gíslason (Nýsköpunarmiðstöð Íslands, 2015).

Chapter 3

Methods

In the following chapter, the methods of this study are explained. The modelling process, the design and the analysis of individual parts of the model are explained. Working fluids, commonly used in ORCs, are analyzed and compared. A case study of the conditions of a greenhouse selected for this study is presented as well as a feasibility study including a cost-benefit analysis for the investment made by the greenhouse owner. Lastly, data from the XRG unit will be presented.

3.1 Geothermal Utilization in Greenhouses in Iceland

A number of greenhouse owners were contacted for this research. Information was gathered on temperatures and mass flow rate of the geothermal fluid used for heating. In addition, a number of greenhouse owners provided information on the percentage of total electricity use used in lighting. This information is important because the government subsidizes the electricity costs for direct lighting in greenhouses (Guðmundsson, 2016). Other use of electricity is paid for at full price and will be discussed in subsection 3.6.1. As seen in Table 3.1 the greenhouses that were studied commonly use geothermal fluid from a nearby borehole at temperatures ranging from 77,5-150°C at a mass flow rate of an average of 8,25 kg/s. After using the fluid, it is usually returned to the ground at a temperature of about 40°C or further used for heating of the facilities.

Table 3.1: Comparison of greenhouses' geothermal resources utilization. *No data found

Greenhouse	Temperature of geothermal fluid [°C]	Mass flow rate from borehole [kg/s]	Percentage of total electricity used for lighting in greenhouses [%]	Source
Ártangi	90	7	80	(Þorgeirsson, 2016)
Gróður	115	2	95	(Jóhannesson, 2016)
Gufuhlíð	96	5-6	99	(Jakobsson, 2016)
Laugaland	100	25-30	90-95	(Bjarnason, 2016)
Friðheimar	94	6	95	(Ármannsson, 2016)
Reykjaflöt	150	*	*	(Stefánsson, 2016)
Hveravellir	95	10	*	(Ólafsson, 2016)
Heiðmörk	100	4	*	(Sævarsson, 2016)
Leirárskógar 1	77.5	3	*	(Matthíasson, 2016)
Leirárskógar 2	60	7	*	(Matthíasson, 2016)
Leirárskógar 3	125	10.5	*	(Matthíasson, 2016)
Average	100,23	8,25	92,3	

Information in Table 3.1 is not based on measured data but are estimated values from the greenhouse owners contacted. It should also be noted that some greenhouses may require less than 100 kW of electricity and therefore, in those applications, this study's unit would not be an appropriate choice.

3.2 Turbine vs. Expander

For smaller ORC units, positive displacement expanders have often been applied, mostly for applications that deliver less than 100 kW of electrical energy. Since this model strives to produce 100 kW it is important to decide whether an expander or a turbine is the better option for this study's model. Both turbines and expanders come in different types. Turbines can be axial, cantilever and radial. Expanders may be of the scroll, piston screw or vane type. The XRG unit, discussed in section 2.4 uses a scroll expander. A scroll expander is a volumetric expander, meaning that the scroll expander uses the expansion work directly by changing the volume of the working chamber. Expanders have a set volume ratio that is then used to acquire the parameters needed in order to deliver a desired amount of energy. Turbines are dynamic, meaning that they convert the vapor's enthalpy to kinetic energy and therefore

the amount of energy delivered can be calculated given set parameters. Different types of expanders can be seen in Figure 3.1 and different types of turbines in Figure 3.2:

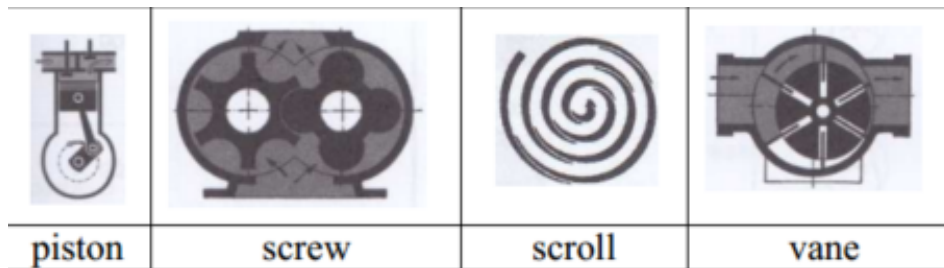


Figure 3.1: A schematic of different types of expanders (Weiß, 2015)

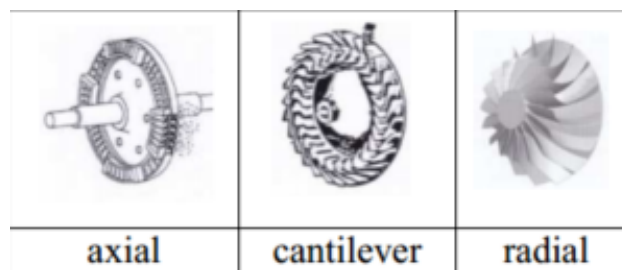


Figure 3.2: A schematic of different types of turbines (Weiß, 2015)

Scroll expanders are more expensive and only smaller temperature differences can be processed efficiently. This is not an issue in the turbine. The scroll expander does have the benefit of being able to operate even though liquid is present in the vapor but this is not considered a deciding factor in this model. They are equally efficient, but the turbine is usually bigger in volume. According to literature, expanders are better for smaller ORC units, such as the XRG unit, but when a higher power output is needed, a higher temperature difference and volume ratios are expected and thus a turbine is a better option (Weiß, 2015) (Tang, 2014). In light of this, a turbine was selected the appropriate choice for this study.

3.3 Modelling

The modelling of the Organic Rankine cycle used for this study was performed in Engineering Equation Solver (EES). EES is an equation solving program that includes a thermodynamic property database for hundreds of substances commonly used in thermodynamic applications (F-Chart Software, 2016). The modelled cycle consists of two heat exchangers (evaporator and condenser), a pump and a turbine.

3.3.1 Cycle States

The cycle is divided in to states 1-8, as seen on Figure 3.3 and detailed below.

Process 1-4 Heat addition in an evaporator

This process includes an evaporator, otherwise known as a boiler, used to boil the working fluid. This process is further divided in to a pre-heater (PH), evaporator (EV) and a super-heater (SH). The working fluid enters the boiler in liquid phase and exits as a superheated vapor.

Process 4-5 Expansion in a turbine

The working fluid, now in its vapor phase, enters the turbine. This is where electricity is produced by the use of a generator.

Process 5-8 Heat rejection in a condenser

This is the condensing state. The working fluid is condensed back to its liquid phase. This process is further divided in to a de-super-heater (DSH), a condenser (C) and a subcooler (SC). The working fluid exits this process as a liquid.

Process 8-1 Compression in a pump

In this state the working fluid is pumped back to the evaporator, completing the cycle.

A schematic of the Organic Rankine Cycle modelled is represented in Figure 3.3. On the left-hand side in Figure 3.3, the heat source for the cycle flows through the evaporator and similarly cold water runs through the condenser as shown on the right side of the diagram. Individual components will be explained in more detail in chapter 2.1.1. States 1 through 8 seen on Figure 3.3 will be used throughout this study in regards to states and processes.

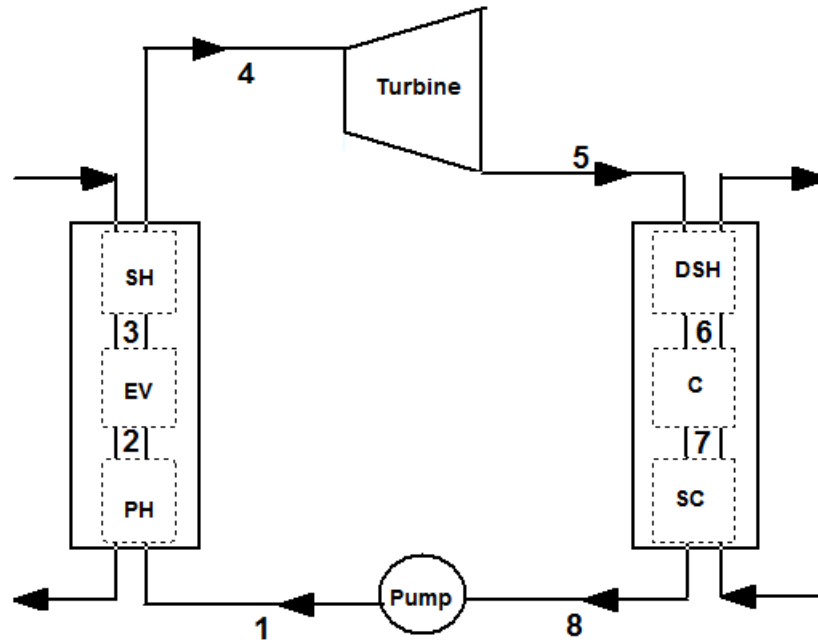


Figure 3.3: A block diagram of an Organic Rankine Cycle

Constants in the model were the inlet temperatures of both the geothermal fluid and the cooling fluid as well as the mass flow rate of the geothermal fluid. Working fluid temperatures at states 2 and 6 were optimized in order to deliver the most net power output. Optimization was performed on the subcool and superheat temperatures, as well. Those values in turn control temperatures at states 4 and 8. Restrains were made for the cooling water's mass flow rate. That mass flow rate has upper bounds of 30 kg/s. A mass flow rate higher than that is not considered realistic even though this value could be altered for different scenarios.

3.3.2 Individual Components

Individual components of the ORC cycle will be explained and analysed in the following subsections; Heat exchangers, pump and turbine.

3.3.2.1 Heat Exchangers

Heat exchangers are devices that allow two fluids to exchange heat without mixing. They are used for various applications like in space heating, air conditioning, power production, waste heat recovery and chemical processing. The three main types of heat exchangers include a concentric tube (double tube), shell and tube and lastly, a plate heat exchanger. The concentric tube heat exchanger is the simplest. It is composed of straight sections of tubing within an outer shell. The shell and tube exchanger has multiple tubes and often uses baffles to increase turbulence. They can be either parallel or counter flow. Parallel flow is where both fluids flow in the same direction and counter flow is where they flow in opposite directions (Moran, Shapiro, Munson, and DeWitt, 2003). Plate heat exchangers (PHE) use a stack of corrugated metal plates in mutual contact, each plate having four ports; two for inlets and two for outlets, one of each for each fluid. Seals are designed to direct the fluids in alternate flow passages. The flow passages are formed by adjacent plates to allow the fluids to exchange heat while passing through alternate channels. The size and number of the plates are dependent on flow rate of fluids, physical properties, pressure drop and temperature. This arrangement produces high turbulence for efficient heat transfer. Figure 3.4 shows a typical plate heat exchanger.



Figure 3.4: A schematic showing a typical plate heat exchanger (Northern Lights. Solar Solutions, 2016).

In this study, plate exchangers are modelled, both for the evaporation and condensation, due to the PHE's ability to produce high turbulence. The high turbulence produces more efficient heat transfer and less flow induced vibrations. Vibration can cause strain on the material. It has no welds and is easily maintained and cleaned (Thulukkanam, 2013).

Evaporator

The purpose of the evaporator is to heat up the working fluid and turn it into vapor. The working fluid enters the evaporator as a compressed liquid and exits as a superheated vapor. The evaporator is further divided into three parts: preheater (PH), an evaporator (EV) and a superheater (SH). These parts are not separate heat exchangers, but only analysed separately for a better heat transfer analysis. In this study, the simplification is made that the process is isobaric, meaning that no pressure losses occur and the pressure is constant through the whole heat exchanger. The preheater heats up the working fluid without it boiling. The phase change occurs in the evaporator as the fluid transforms from its liquid phase and becomes gaseous without any temperature or pressure changes. The vapor quality and the enthalpy changes during the evaporation. In the final part of the heat exchanger, the superheater, the vapor is superheated to increase its energy content. The value of the superheat was optimized in the model. The vapor quality of the working fluid is assumed to be 0 as it exits the preheater, 1 after the evaporator and superheated after the superheater.

On the warmer side of the evaporator geothermal fluid is used and working fluid flows on the colder side. The geothermal fluid heats the working fluid up to the desired temperature. The geothermal fluid enters the heat exchanger at the same side as the outlet of the working fluid (counter flow). This warm geothermal fluid is assumed to enter the heat exchanger at a temperature of 100,23°C and exit at 48,52°C although these numbers can, and will, be easily modified to accommodate other conditions. This inlet temperature is the medium value calculated in section 3.1 and correspond to the temperature of the geothermal fluid used by greenhouses. The temperature distribution over the process 1-4, the evaporator, can be seen in Figure 3.5. The correlating mass flow rate of the working fluid is 8,16 kg/s. The dashed

line representing the warmer fluid, in this case, the geothermal fluid, and the solid line represents the colder fluid, the working fluid.

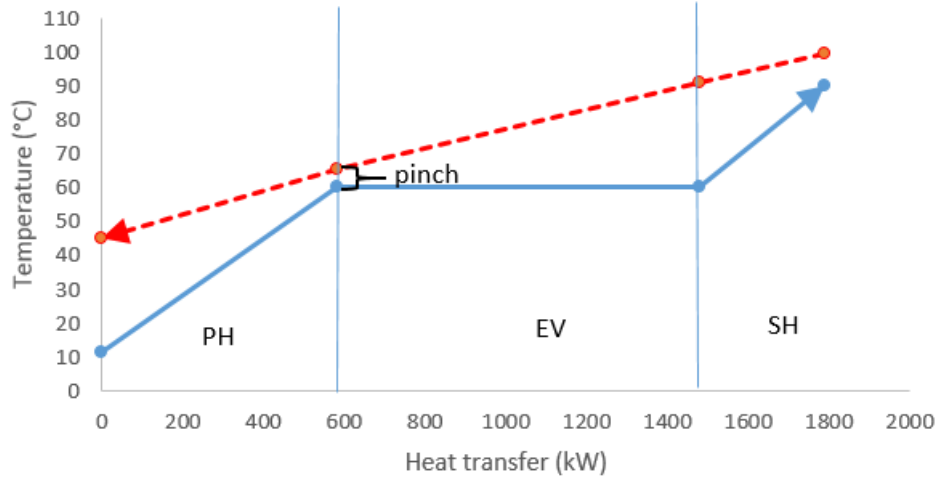


Figure 3.5: A graph showing the temperature and heat transfer correlation in the evaporator

Condenser

The condenser's purpose is to cool down the vapor, condense it, and to keep the pressure down as the fluid exits the condenser. Its function is like the evaporator but in reverse. It can be further divided into a de-super heater (DSH), a condenser (C) and a sub-cooler (SC). These parts are not separate heat exchangers, but only analysed separately for a better heat transfer analysis. In this study the process is assumed to be isobaric, meaning that the pressure is constant through the whole heat exchanger. The de-super heater cools the working fluid down to 20,55°C from 60,23°C. In the condensing part, the vapor is condensed to a liquid phase without the temperature or pressure changing similar to the evaporator. The vapor quality and enthalpy of the fluid changes. In the sub-cooler, the fluid is further cooled. The value of subcooling was optimized in the model.

On the colder side of the condenser it is assumed that a fresh water source is used. This source is assumed to be a nearby creek with plenty of running water. The temperature at the cold water inlet is assumed to be 5°C, and it exits the heat exchanger at a corresponding temperature of 18,18°C. The temperature distribution over the sub-processes can be seen in

Figure 3.6. The corresponding mass flow rate of the working fluid is 8,16 kg/s. The dashed line representing the warmer fluid, in this case the working fluid and the solid line represents the colder fluid, the cooling water.

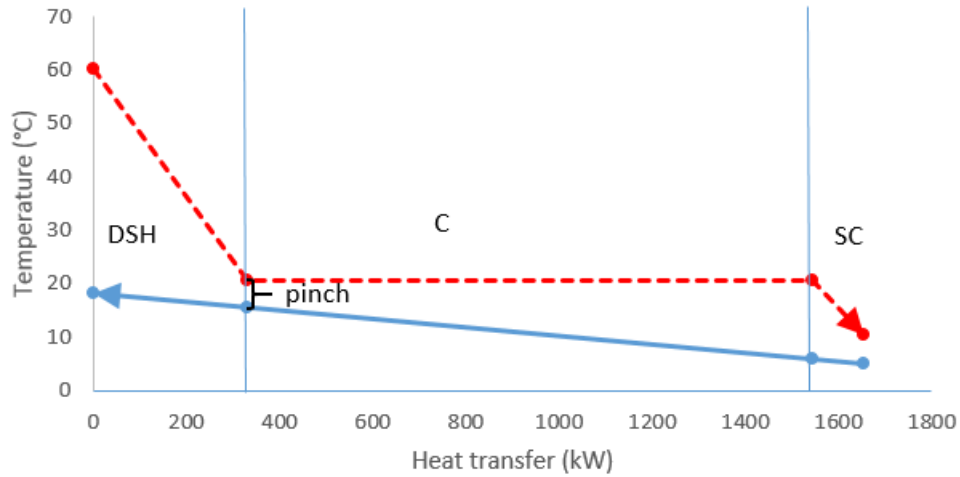


Figure 3.6: A graph showing the temperature and heat transfer correlation in the condenser

Heat Exchanger Analysis

To predict the performance of heat exchangers, total surface area must be related to the temperatures involved, fluid flow rates and the heat transfer coefficient.

Pinch

Pinch point technology is based on the first and second laws of thermodynamics. The pinch point is the smallest temperature difference between the colder and warmer fluids. The smaller the pinch, the higher the heat transfer coefficient (Tewari, Agrawal, and Arya, 2014). For this study, the pinch was set at 5 °C both for the condenser and the evaporator. These values are set as constants in the model, meaning that the temperatures of the fluids are dependent on each other. These values are common pinch values in heat exchangers in small scale ORC units according to literature (Georges, Declaye, Dumont, Quoilin, and Lemort, 2013), (Quoilin, 2008), (Declaye, Quoilin, and Lemort, 2010). In this study's model

the pinch point occurs at state 2 in the evaporator and at state 6 in the condenser. The pinch value is visually represented in Figures 3.5 and 3.6.

Energy Balance in Heat Exchangers

Energy balance refers to the first law of thermodynamics. The law states that energy can neither be destroyed nor created, only transformed from one form to another. This applies to heat exchangers analysis assuming that heat exchangers are isolated systems and all energy is stored within the system (Moran et al., 2003).

Energy in to a system therefore equals energy out of that same system. Energy out is the mass flow rate of the working fluid multiplied with it's enthalpy difference over the heat exchanger. Energy in refers to the mass flow rate of the cooling fluid multiplied with it's enthalpy difference over the heat exchanger. For the evaporator the energy in is the mass flow rate of the geothermal fluid multiplied with it's enthalpy difference and energy out is the mass flow rate of the working fluid multiplied with it's enthalpy difference.

This relationship is represented by Equations (3.1) and (3.2) for the condenser and the evaporator, respectively.

$$\begin{aligned}\dot{Q}_{in} &= \dot{Q}_{out} \\ \dot{m}_{wf}(h_5 - h_8) &= \dot{m}_c(h_{cout} - h_{cin})\end{aligned}\tag{3.1}$$

$$\begin{aligned}\dot{Q}_{out} &= \dot{Q}_{in} \\ \dot{m}_{wf}(h_4 - h_1) &= \dot{m}_h(h_{hin} - h_{hout})\end{aligned}\tag{3.2}$$

\dot{m}_{wf} being the mass flow rate of the working fluid, \dot{m}_c is the mass flow rate of the cooling water and \dot{m}_h for the geothermal fluid, all in kg/s. h_5 , h_8 , h_4 and h_1 are enthalpies for states 5, 8, 4 and 1 respectively. h_{cout} and h_{cin} represent the enthalpies for cooling water at the inlet and outlet of the heat exchangers and h_{hin} and h_{hout} represent the enthalpies for the geothermal fluid's inlet and outlet. All enthalpies are in the unit kJ/kg.

Log Mean Temperature Difference (LMTD)

The logarithmic mean temperature difference is used to determine the appropriate temperature difference in counter flow heat exchangers. It is the logarithmic average of the temperature difference between the warmer and cooler inlet and outlet temperatures. The log mean temperature difference ($\Delta T_{lm,boil}$) is represented by Equation (3.3) for the evaporator

$$\Delta T_{lm,boil} = \frac{\Delta T_2 - \Delta T_1}{\ln \frac{\Delta T_2}{\Delta T_1}} \quad (3.3)$$

ΔT_1 and ΔT_2 are the endpoint temperatures, meaning the temperature differences at each end of the heat exchanger. Those temperatures are represented by Equations (3.4) and (3.5):

$$\Delta T_1 = T_{hin} - T_4 \quad (3.4)$$

$$\Delta T_2 = T_{hout} - T_1 \quad (3.5)$$

ΔT_1 and ΔT_2 are the endpoint temperatures, T_{hin} and T_{hout} are the temperatures of the warmer fluid at the inlet and outlet of the evaporator and T_1 and T_4 are the temperatures at states 1 and 4, respectively. The location of these temperatures is shown in Figure 3.7

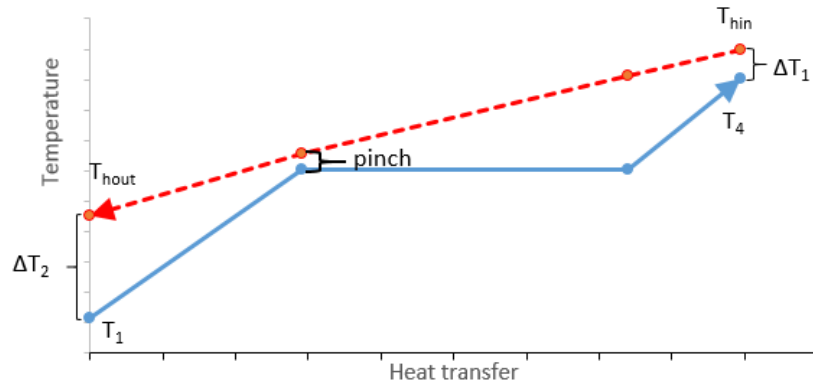


Figure 3.7: Location of temperatures used in the LMTD calculation for the evaporator

The $\Delta T_{lm,cond}$ is the LMTD of the condenser and is represented in a similar manner in Equations (3.6), (3.7) and (3.8) :

$$\Delta T_{lm,cond} = \frac{\Delta T_4 - \Delta T_3}{\ln \frac{\Delta T_4}{\Delta T_3}} \quad (3.6)$$

$$\Delta T_3 = T_8 - T_{cin} \quad (3.7)$$

$$\Delta T_4 = T_5 - T_{cout} \quad (3.8)$$

ΔT_3 and ΔT_4 are the endpoint temperatures, T_{cin} and T_{cout} are the temperatures of the colder fluid at the inlet and outlet of the condenser and T_5 and T_8 are the temperatures at states 5 and 8, respectively. The location of these temperatures is shown in Figure 3.8

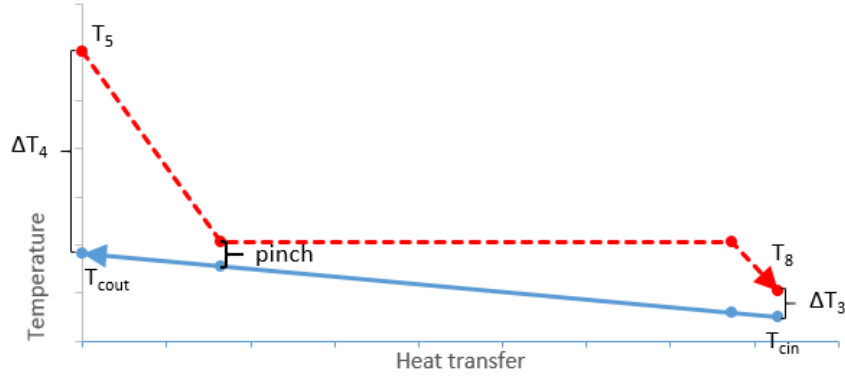


Figure 3.8: Location of temperatures used in the LMTD calculation for the condenser

This LMTD value has been widely used in heat transfer analysis, however, this value does not accept phase change. A correction factor has to be applied in order to better represent this model's heat exchangers. This correction factor depends on the inlet and outlet temperatures of the fluids (Bergman, Lavine, Incropera, and DeWitt, 2011). Temperature ratios P and R are calculated by Equations (3.9) and (3.10) for the evaporator

$$P_{boil} = \frac{T_4 - T_1}{T_{hin} - T_{hout}} \quad (3.9)$$

$$R_{boil} = \frac{T_{hin} - T_{hout}}{T_4 - T_1} \quad (3.10)$$

P and R are the temperature ratios. T_{hin} and T_{hout} are the temperatures of the geothermal fluid at the inlet and outlet of the evaporator. T_4 and T_1 are the temperatures of the working fluid at states 4 and 1, respectively.

Similarly for the evaporator Equations (3.11) and (3.12) are used:

$$P_{cond} = \frac{T_{cout} - T_{cin}}{T_5 - T_8} \quad (3.11)$$

$$R_{cond} = \frac{T_5 - T_8}{T_{cout} - T_{cin}} \quad (3.12)$$

P and R are the temperature ratios. T_{cin} and T_{cout} are the temperatures of the geothermal fluid at the inlet and outlet of the evaporator. T_5 and T_8 are the temperatures of the working fluid at states 5 and 8, respectively.

These ratios are then used to estimate the correction factor, F, using Figure 3.9.

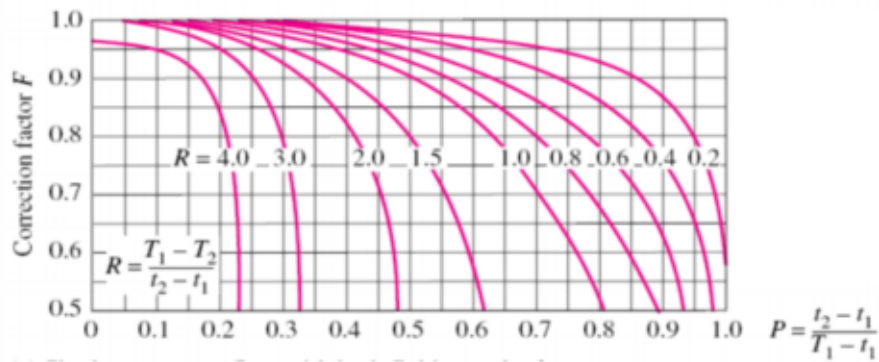


Figure 3.9: Correction factor chart for cross flow heat exchangers. T referring to the hotter fluid's temperatures, t referring to the colder fluid's temperatures and subscripts 1 and 2 representing inlet and outlet. (Bergman, Lavine, Incropera, and DeWitt, 2011).

This factor is then multiplied with the LMTD differences. For this model's temperatures the factor is approximately 0,8 for both heat exchangers. The corrected value of the LMTD temperatures are used in all further calculations.

Overall Heat Transfer Coefficient

The overall heat transfer coefficient is useful to evaluate the performance of the heat exchanger. Equation (3.13) represents this value.

$$U = \frac{\dot{Q}}{A\Delta T_{lm}} \quad (3.13)$$

U is the overall heat transfer coefficient in $\text{kW/m}^2 \text{ }^\circ\text{C}$. \dot{Q} is the heat flux in Watts, A is the total heat transfer area in m^2 of the heat exchanger and ΔT_{lm} is the corrected log mean temperature difference in $^\circ\text{C}$. Those temperatures were calculated in Equations (3.3) and (3.6) and corrected with the correction factor estimated from Figure 3.9. According to DiPippo (DiPippo, 2012) the approximate values of the overall heat exchanger coefficient, for this case, are 0,45 - 0,85 ($\text{kW/m}^2 \text{ }^\circ\text{C}$) for the condenser and 0,17 - 0,85 ($\text{kW/m}^2 \text{ }^\circ\text{C}$) for the evaporator. A high heat transfer coefficient is ideal since it improves the performance of the heat exchanger. The average values of those heat transfer coefficients are used to estimate the heat transfer area and then for calculating the heat transfer area by Equation (3.13) (DiPippo, 2012).

3.3.2.2 Pump

The pump is used to supply fluid at a sufficient pressure from the condenser to the evaporator. In this process, the temperature increase is a trivial amount, but the pressure is raised considerably. The pump consumes power and to estimate the power needed, enthalpies on each state (1 and 8) are needed. That difference is multiplied by the mass flow rate of the working fluid as seen in Equation (3.14)

$$\dot{W}_{\text{pump}} = \dot{m}_{\text{wf}}(h_1 - h_8) \quad (3.14)$$

\dot{W}_{pump} is the pump work in kW, \dot{m}_{wf} is the mass flow rate of the working fluid in kg/s and h_1 and h_8 are the outlet and inlet enthalpies in kJ/kg, respectively.

3.3.2.3 Turbine

A turbine is a device where work is produced as a result of vapor passing through a set of blades attached to a shaft that is free to rotate. In this process, the working fluid drops in pressure and temperature. To calculate the power output, enthalpies on each side (4 and 5)

are needed. That difference is multiplied by the mass flow rate of the working fluid as seen in Equation (3.15)

$$\dot{W}_{turb} = \dot{m}_{wf}(h_4 - h_5) \quad (3.15)$$

\dot{W}_{turb} is the turbine work in kW, \dot{m}_{wf} is the mass flow rate of the working fluid in kg/s and h_4 and h_5 are the inlet and outlet enthalpies in kJ/kg, respectively.

Net Power Output

The net total power output, the power that is delivered by the unit is simply the difference between \dot{W}_{turb} and \dot{W}_{pump} calculated in Equations (3.15) and (3.14), respectively. The net power output is represented by Equation (3.16).

$$\dot{W}_{cycle} = \dot{W}_{turb} - \dot{W}_{pump} \quad (3.16)$$

Efficiencies

Realistically the power output is not as high as calculated in the previous section. Both the turbine and the pump deliver less than theoretically calculated. The correct approach is to assign an isentropic efficiency value to both the turbine and the pump. Those values vary slightly according to literature and it is safe to assume values of 80% for both the turbine and the pump (Harada, 2010), (Lee, Yang, Park, Lee, and Park, 2015), (Seta, Andreasen, Pierobon, Persico, and Hagaling, 2015). Equations (3.17) and (3.18) show the power values including the efficiency.

$$\dot{W}_{turb,a} = \dot{W}_{turb} * \eta_{turb} \quad (3.17)$$

$$\dot{W}_{pump,a} = \dot{W}_{pump} * \eta_{pump} \quad (3.18)$$

η_{turb} is the isentropic efficiency of the turbine, η_{pump} is the isentropic efficiency of the pump and $\dot{W}_{turb,a}$ and $\dot{W}_{pump,a}$ are the actual power output and input of the turbine and the pump, respectively.

Performance of power cycles is usually expressed by thermal efficiency (η_{th}). Thermal efficiency is the ratio of net power output and heat transfer rate of the evaporator. The thermal efficiency is expressed by Equation (3.19) (Moran et al., 2003):

$$\eta_{th} = \frac{\dot{W}_{turb} - \dot{W}_{pump}}{\dot{Q}_{boil}} = \frac{\dot{W}_{cycle}}{\dot{Q}_{boil}} \quad (3.19)$$

η_{th} is the thermal efficiency, \dot{W}_{turb} is the work output of the turbine, \dot{W}_{pump} is the power input of the pump and \dot{Q}_{boil} is the heat transfer rate of the evaporator. All in units in kW.

Another parameter commonly used to describe the performance of the ORC is the back work ratio (BWR) which is defined as the ratio of the pump work input and the work done by the turbine. A large value of BWR indicates that the work done in the pump is large, and a value above 1 would mean that the net power output is negative. Ideally this value should be as low as possible. This ratio is demonstrated in Equation (3.20) (Moran et al., 2003):

$$BWR = \frac{\dot{W}_{pump}}{\dot{W}_{turb}} \quad (3.20)$$

BWR is the back work ratio, \dot{W}_{turb} is the power output from the turbine, including efficiency, and \dot{W}_{pump} is the power input to the pump, including efficiency.

3.4 Comparable Commercial ORC Units

A few comparable ORC units were researched according to important parameters. Dimensions, prices and turbine or expander choices are listed in Table 3.2, and geothermal fluid's temperatures and working fluid selections are listed in Table 3.3. These units are all comparable in regards to net power output and all sizes include all components, heat exchangers, turbine/expander, pump, and piping.

Table 3.2: Commercial ORC units' parameters, comparable to the case in this study

*No data found					
Model	Total Volume [m ³]	Power Output [kW]	Turbine/ Expander	Price MISK	Source
Electrotherm 6500	25,92	110	Expander	33	(Electrotherm, 2016)
Enogia ENO100-LT	9,07	100	Turbine	27	(Enogia, 2016)
E-Rational ORC-1000	13,79	110	Expander	*	(E-Rational, 2015)
Zuccato ZE-100-LT	29,78	100	Turbine	*	(Zuccato Energia, 2016)

Table 3.3: Commercial ORC units' parameters, cont.

*No data found			
Model	Temperature range of geothermal fluid [°C]	Working fluid	Source
Electrotherm 6500	77-122	R245fa	(Electrotherm, 2016)
Enogia ENO100-LT	60-100	R245fa	(Enogia, 2016)
E-Rational ORC-1000	85-150	R245fa	(E-Rational, 2015)
Zuccato ZE-100-LT	60-165	*	(Zuccato Energia, 2016)

These units are very different in size but all have similar temperature ranges of the geothermal fluid. Most of them use R245fa as a working fluid. Two of them listed their prices, which include all parts of the ORC unit as well as the working fluid. These prices are similar but the units from E-Rational and Zuccato did not list prices of their units.

3.5 Working Fluids

Working fluid selection for ORC cycles can be a complex task and has been treated in many articles (Datla and Brasz, 2012) (Quoilin, Declaye, Legros, Guillaume, and Lemort, 2012). It is the author's opinion that the most relevant parameters of the working fluid for the scope of this thesis are as follows:

- Critical temperature and pressure

Higher critical temperatures and pressures often indicate higher efficiency.

- Boiling point

Boiling points are lower in the working fluid than in the heat source fluid. This allows for the fluid to boil at a lower temperature than in conventional Rankine steam cycles.

- Atmospheric life time

Atmospheric life time is the number of years it takes a substance to leave the atmosphere

- Ozone depletion potential (ODP)

Ozone depletion potential refers to the fluids ability to damage the ozone layer. The lower, the better applies in this case, and most refrigerants have an ODP value close to zero.

- Global warming potential (GWP)

Global warming potential refers to the amount of global warming caused by the working fluid measured in CO₂ over a period of 100 years. Ideally, this number should be under 1000.

- Flammability (LFL)

Flammability is measured with a parameter called Lower Flammability Limit (LFL). This refers to the lower end concentration of a flammable solvent in ambient air when the mixture can ignite at a given temperature and pressure.

- Toxicity

Toxic fluids have a negative impact on the environment or damaging effect on organisms (Nouman, 2012).

A vast amount of working fluids have been researched but with regards for this study nine different working fluids were tested and compared. These are fluids commonly used in Organic Rankine Cycles (Datla and Brasz, 2012). These fluids were tested in the model, changing only the fluid parameter, with the conditions seen in Figure 3.10. The main inputs used are: Geothermal resource inlet temperature (T_{hin}) is set at 100,23 °C and the cold water's inlet temperature (T_{cin}) is set to 5 °C. The mass flow rate of the geothermal resource is set at 8,25 kg/s which in turn controls the mass flow rates of both the working fluid and the cooling water. The inlet temperatures and the flow rate are the average values from the

researched greenhouses in section 3.1. A schematic of the model including the conditions stated above is represented by Figure 3.10.

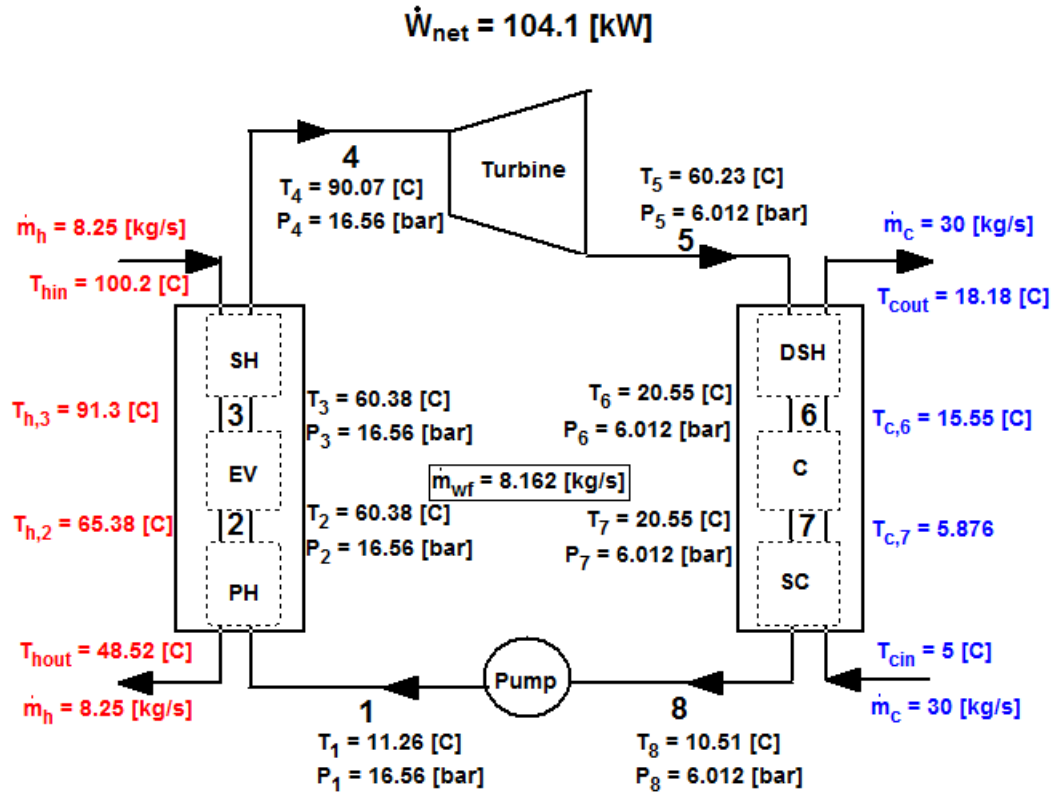


Figure 3.10: The cycle including conditions chosen for working fluid comparison

Working fluid properties are compared in Tables 3.4, 3.5 and 3.6

Table 3.4: Physical properties of selected working fluids (Nouman, 2012)

Working fluid	Critical Temperature [°C]	Critical pressure [bar]	Boiling point at 1 bar [°C]
D4	313,35	13,35	175,35
D5	346	11,6	210,9
Isopentane	187,2	33,78	27,8
R123	183,68	36,67	27,8
R1234yf	94,7	33,8	-29,5
R1234ze(E)	109,4	36,4	-19
R134a	101	40,59	-26
R245fa	154	36,51	15,14
Toluene	318,6	41,26	110,6

Table 3.5: Environmental properties of selected working fluids (Nouman, 2012) (Navea, Young, Xu, Grassian, and Stanier, 2011) *No data found

Working fluid	Atmospheric life time	Ozone Depletion potential (ODP)	Global warming potential (GWP)
D4	11,5	*	*
D5	7,5	*	*
Isopentane	0,009	0	20
R123	1,3	0,01	77
R1234yf	0,029	0	0
R1234ze(E)	0,045	0	6
R134a	14,6	0	1300
R245fa	7,7	0	1050
Toluene	0,004	0	0

Table 3.6: Safety data of selected working fluids (Nouman, 2012) (Datla and Brasz, 2012)

Working fluid	Flammability (LFL)	Toxicity
D4	Moderate	Low
D5	Moderate	Low
Isopentane	High	Low
R123	No	High
R1234yf	Low	Low
R1234ze(E)	Low	Low
R134a	No	Low
R245fa	No	High
Toluene	High	Low

To predict the performance of the working fluids the net electricity output was calculated for each fluid. Comparisons can be seen in Figure 3.11 for the net power output (calculated by Equation(3.16)) and on Figure 3.12 for the cycle's thermal efficiency. The thermal efficiency is calculated with Equation (3.19).

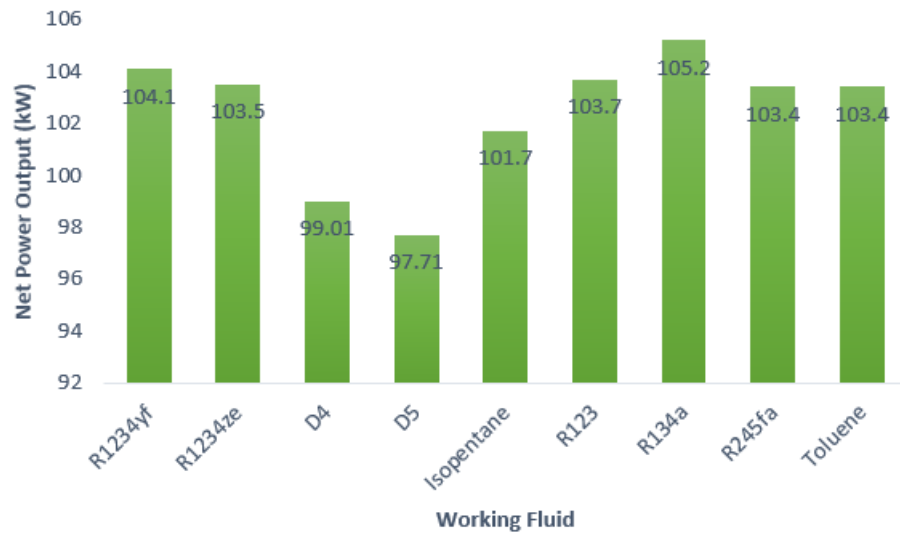


Figure 3.11: Net Power output of different working fluids

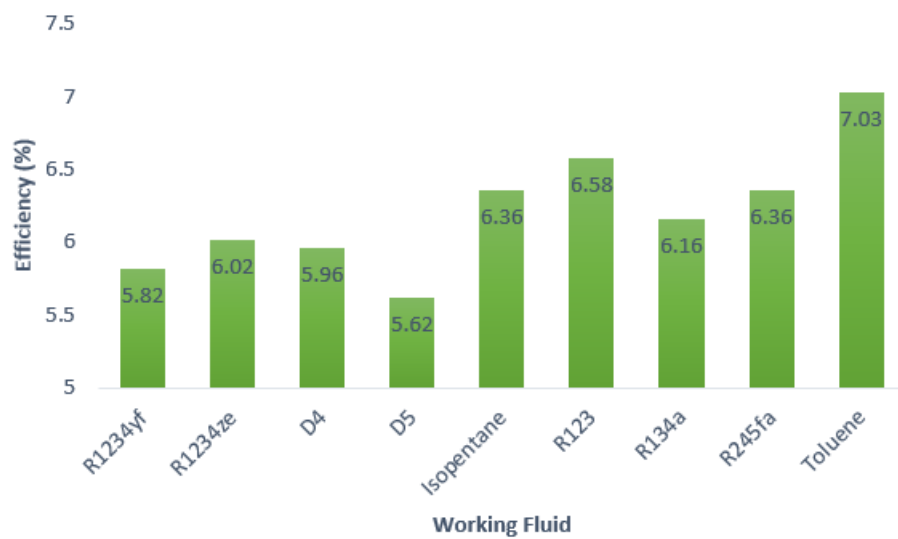


Figure 3.12: Cycle thermal efficiency of different working fluids

T-s (temperature-entropy) diagrams of the selected fluids including pressures can be seen in Figures 3.13, 3.14, 3.15 and 3.16.

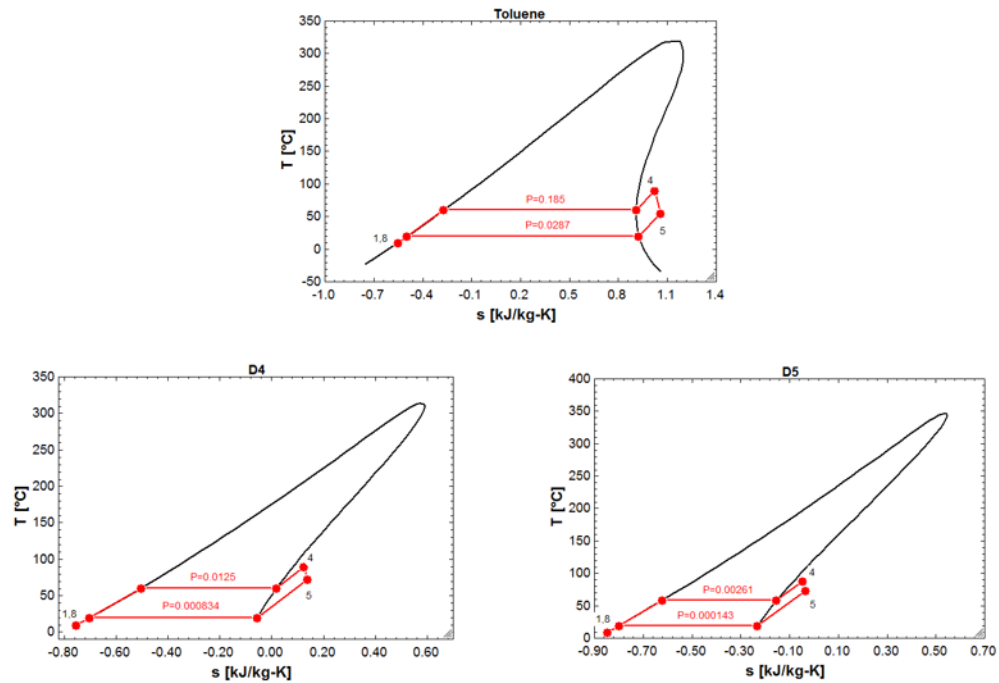


Figure 3.13: T-s diagrams of Toluene on top, D4 on the left and D5 on the right

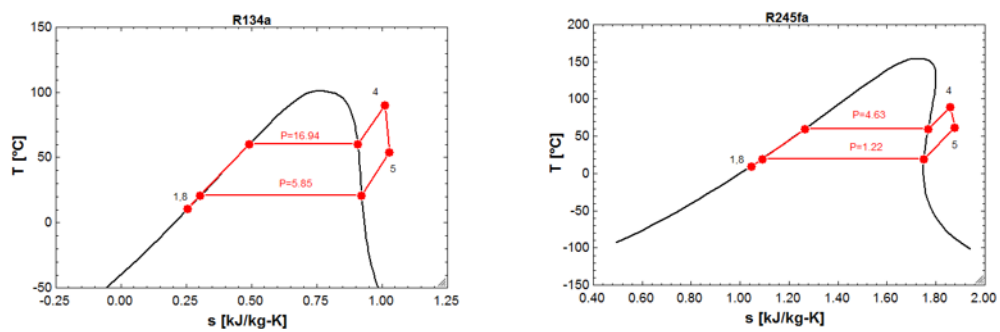


Figure 3.14: T-s diagrams of R134a on the left and R245fa on the right

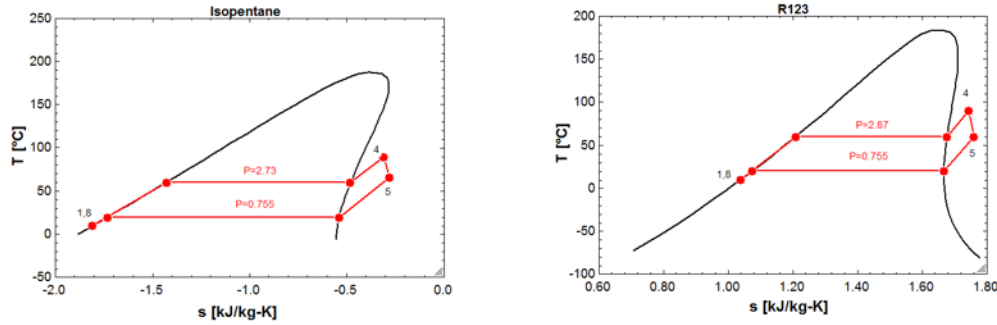


Figure 3.15: T-s diagrams of Isopentane on the left and R123 on the right

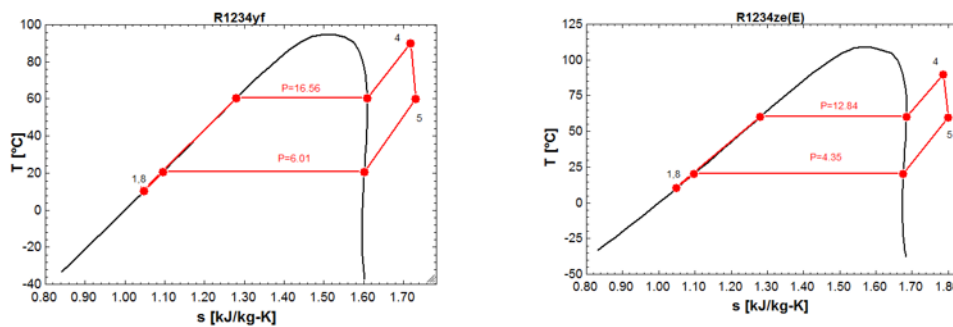


Figure 3.16: T-s diagrams of R1234yf on the left and R1234ze(E) on the right

The working fluid selected, based on discussed properties, is R1234yf. R1234yf has an appropriate boiling point, a low GWP, low toxicity and flammability and has a fair net power output and efficiency. This will be further discussed in chapter 4 and chapter 5.

3.6 Economic Feasibility

To decide if this project is worth investing in for the greenhouse owner it is necessary to conduct an economic feasibility study. In the following sections a detailed analysis of the prices involved, as well as the benefits, will be listed and compared to conclude whether or not this is a risk worth taking.

It is assumed that the greenhouse owner will have to take a loan to cover the costs of the unit. The main parameters needed for the following calculations are interest rates on that loan. The interest rates assumed are the average values according to the Central Bank of Iceland (Seðlabanki Íslands, 2016).

3.6.1 Electricity Prices for Greenhouses in Iceland

The Icelandic government subsidizes the distribution of the electricity bought by the greenhouse owner and used for lighting. In rural areas, the subsidy covers 92% of the distribution costs and in urban areas the subsidy is 87% (Guðmundsson, 2016). The greenhouse owners pay a set fee to the electricity producer. This fee ranges from 6,70 to 6,99 ISK/kWh depending on the vendor. The distribution fee ranges from 6,03 to 7,55 ISK/kWh for urban areas and 9,32 to 9,57 ISK/kWh for rural areas. Including the subsidy, those prices drop to a range of 0,78 to 0,98 ISK/kWh for urban areas and 0,75 to 0,77 ISK/kWh for rural areas (Orkusetur, 2016). From those numbers, the average greenhouse owner pays a total of 7,7 ISK/kWh for their electricity. This is only valid for direct lighting for the plants/vegetables as all other electricity use such as other lighting, refrigerators and other possible machinery and appliances, is paid for in full without subsidization. The price the greenhouse owner pays for electricity that is not subsidized is on average 14,2 ISK/kWh (Orkusetur, 2016). Table 3.7 lists the prices of different vendors and Table 3.8 displays the prices before and after subsidies of different distributors.

Table 3.7: Electricity sellers price of electricity (Orkusetur, 2016)

Electricity producer	Price per kWh (ISK/kWh)
Fallorka	6,78
HS Orka	6,94
Orka Náttúrunnar	6,80
Orkubú Vestfjarða	6,70
Orkusalan	6,99
Rafveita Reyðafjarðar	6,70

Table 3.8: Electricity distributors price of distribution (Orkusetur, 2016) (Guðmundsson, 2016)

Electricity distributor	Region	Price per kWh [ISK/kWh]	Subsidy for distribution [%]	Price after subsidy [ISK/kWh]
HS Orka	Urban	6,67	87	0,87
Norðurorka	Urban	6,03	87	0,73
OR	Urban	7,55	87	0,98
Orkubú Vestfjarða	Rural	9,32	92	0,75
Orkubú Vestfjarða	Urban	6,84	87	0,89
Rafveita Reyðafjarðar	Urban	6,56	87	0,85
Rarik	Rural	9,57	92	0,77
Rarik	Urban	6,46	87	0,84

3.6.2 Cost Benefit Analysis

Cost Benefit Analysis (CBA) is a decision-making tool for businesses. The benefits of a given situation are summarized, and then the costs of that situation are subtracted. In this case, the business owner is the greenhouse owner. The greenhouse owners' benefits would be the amount saved on electricity and his/her costs are the price of the ORC unit as well as operations and maintenance costs (O&M).

Prices of installed ORC units of this scale range from 20 - 34 million ISK (Arvay, Muller, Ramdeen, and Cunningham, 2011). For this analysis, the average value of those numbers, 27 million ISK, will be used for all further calculations. For simplification, this number is the assumed price of the ORC unit, including installation, labor, any possible transportation as well as the working fluid. The price for this study's unit is therefore 27 million ISK.

Besides the price assumption, it will be assumed that the greenhouse owner will take a loan for the unit. If he/she decides to take a 10-year loan with a 7,3% interest for the full amount he/she will pay in total just over 40 million back over that period (Seðlabanki Íslands, 2016). That amount will be calculated with Equation (3.24) in subsubsection 3.6.2.1. It should be noted that this is a conservative assumption and the payback would be considerably lower if he/she could finance it him-/herself, either partly or in total, or if he/she decided to pay up the loan in a shorter time. In addition to paying for the unit, the greenhouse owner will have to pay a certain amount per year in operations and maintenance (O&M) costs. This

cost is assumed to be around 600.000 ISK/year. This is an average value commonly used as an estimation for ORC technologies and includes maintenance of the unit as well as the borehole and any machinery that might be needed for the cooling water (Energy Technology Network, 2010) (Bombarda, 2016) (David, Michel, and Sanchez, 2011) (Infinity Turbine, 2016). The borehole is already drilled and is commonly owned by the greenhouse owner, therefore drilling costs are not included. It is expected that the machine will run for a lifetime of about 15 years. Since the borehole is already in place, the cost of the unit and the O&M costs are the only costs associated with this unit, no drilling is required. On the benefits side, the only benefits will be the amount saved on electricity. As previously mentioned the average greenhouse owner pays on average 7,7 ISK/kWh for direct lighting and 14,2 ISK/kWh for other electricity use. According to a few greenhouse owners, their percentage of electricity use for direct lighting ranges from 80-99% of their total electricity use. Using the average number of 92,3% a typical greenhouse farmer pays a total of 8,2 ISK/kWh. Calculations presented in Equation (3.21) below

$$\text{Price} = 92,3\% \cdot 7,7 \text{ [ISK/kWh]} + 7,7\% \cdot 14,2 \text{ [ISK/kWh]} = 8,2 \text{ [ISK/kWh]} \quad (3.21)$$

This is the number used in further calculations as the price that the greenhouse owner pays for their total use of electricity.

The ORC unit is expected to produce 100 kW of electricity, and in order to calculate the amount saved per year, those quantities must be multiplied by the number of hours per year as seen in Equation (3.22)

$$\text{Benefits} = 100 \text{ [kW]} \cdot 8,2 \text{ [ISK/kWh]} \cdot 8760 \text{ [h/year]} = 7.183.200 \text{ [ISK/year]} \quad (3.22)$$

A capacity factor is the ratio of the actual output of a power plant to its output if operated at a full nameplate capacity over a given time (IEA Geothermal, 2010). For the purpose of this study it is assumed that this factor is 0,9 (90%). Including that the benefits go down to 6.464.880 ISK/year.

3.6.2.1 Net Present Value

Net Present Value (NPV) is the difference between the present value of cash inflows and the present value of cash outflows. A negative NPV implies the investment should not be made and a positive NPV implies a good investment. The larger the value, the better the investment (Arshad, 2012). The NPV is calculated with Equation (3.23)

$$\sum_{n=0}^{15} \frac{C_n}{(1+r)^n} \quad (3.23)$$

n represents the years, in this case n=15 years, the estimated lifetime of the unit C_n is the cash flow on year n, and r is the discount rate. As previously stated the greenhouse owner will take a bank loan for 27 million ISK for 10 years. This loan is assumed to have 7,3% interests (Seðlabanki Íslands, 2016). Loan management fees are assumed to be 2% or 540.000 ISK. Other loan costs will be disregarded since they are considered minimal compared to the total loan amount.

To calculate the amount paid monthly from the loan Equation (3.24) is used:

$$P = \frac{\frac{r}{1200} B}{(1 - (1 + r)^{-N})} \quad (3.24)$$

P is the monthly payment, B is the loan amount, r is the interest and n is the number of payments ($N=n*12$). In this case the payment is 317.680,9 ISK/month. Yearly that amounts to 3.812.170 ISK/year. This is the cost part of the analysis. Another part of the costs are the O&M costs that are 600.000 ISK/year. The total cost per year, in the first ten years, is therefore 4.412.170 ISK/year.

3.7 Case Study - Friðheimar

The purpose of this case study is to test the model in a realistic environment. The greenhouse selected for the case study is Friðheimar.

Friðheimar is a greenhouse located in the south of Iceland. It has been in business since 1946, but since 1995 by the current owners. It specializes in tomatoes but the owners, Knútur and Helena, run a restaurant and raise horses as well. The greenhouses' heating needs are provided by a nearby borehole, Reykholtshver, located about 300 meters from the greenhouse. The borehole used to heat up their facilities is owned by Friðheimar and the neighbouring homes and businesses. (Friðheimar, 2016). The geothermal fluid provided to the Friðheimar Greenhouse is at 94 °C and has a current mass flow rate of 6 kg/s. Reykholtshver produces 14 kg/s and other boreholes in that area produce 12 and 15 kg/s. These three holes service the area, including Friðheimar, other businesses and homes (Ármannsson, 2016). Location of Friðheimar is seen in Figure 3.17 and the location of the greenhouse and the borehole can be seen in Figure 3.18



Figure 3.17: Location of Friðheimar Greenhouse (marked with a star) (Orkustofnun, 2016)



Figure 3.18: Location of Friðheimar Greenhouse and the borehole Reykholtshver (marked with a star) (Google Maps, 2016)

This greenhouse was chosen due to easy access to data and cooperation with the owners and employees. Many assumptions were made including that the cooling water will be from a nearby creek at the desired temperature of 5 °C. The working fluid used is the one chosen in section 3.5, R1234yf. It is also assumed that the returned geothermal fluid can be further used for heating up the greenhouse. Conditions chosen for the case study can be seen in the block diagram in Figure 3.19

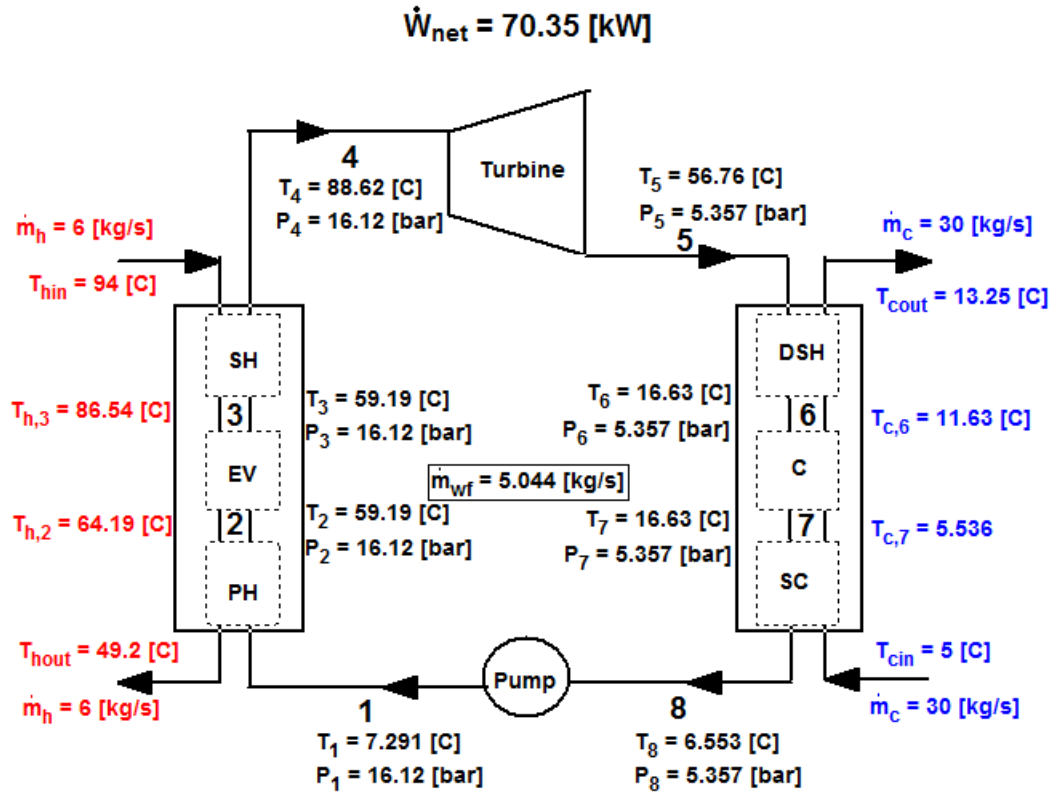


Figure 3.19: A schematic of the model's ORC cycle including temperature and mass flow rate of Friðheimar's geothermal resource

From these modelling conditions, the ORC cycle produces 70,35 kW at a thermal efficiency of 6,25%. This is a lower power output than the model's intent but this result can be explained by a lower than average mass flow rate that is a controlling factor in power output.

Friðheimar uses about 95% of its electricity use for direct lighting. As discussed in section 3.6 that part is subsidized by the government and using Equation (3.25):

$$\begin{aligned} \text{Case Study Price} = & \\ 95\% \cdot 7,7 \text{ [ISK/kWh]} + 5\% \cdot 14,2 \text{ [ISK/kWh]} = 8,03 \text{ [ISK/kWh]} & \quad (3.25) \end{aligned}$$

The calculated price paid by Friðheimar is 8,03 ISK/kWh. The benefits are then calculated using Equation (3.26):

$$\begin{aligned} \text{Case Study Benefits} = \\ 70,35 \text{ [kW]} \cdot 8,03 \text{ [ISK/kWh]} \cdot 8760 \text{ [h/year]} = 4.948.616 \text{ [ISK/year]} \end{aligned} \quad (3.26)$$

Assuming a 90% capacity factor this number goes down to 4.453.754 ISK/year. The costs from the Friðheimar greenhouse owners are the same as used in calculations in section 3.6.

3.8 Model Comparison with the XRG Unit

Measurements were done on the XRG unit discussed in section 2.4 by Jón Matthíasson at the Innovation Center Iceland in December 2015.

All measurements were done over a time period of 50 minutes, and performed using the open source software Scilab for numerical computation (Scilab Enterprises, 2015). For this study the data was gathered, adjusted accordingly and plotted.

The geothermal fluids inlet temperature was measured on average 73,6 °C. This measurement is represented by Figure 3.20 and the corresponding outlet temperatures are shown on Figure 3.21.

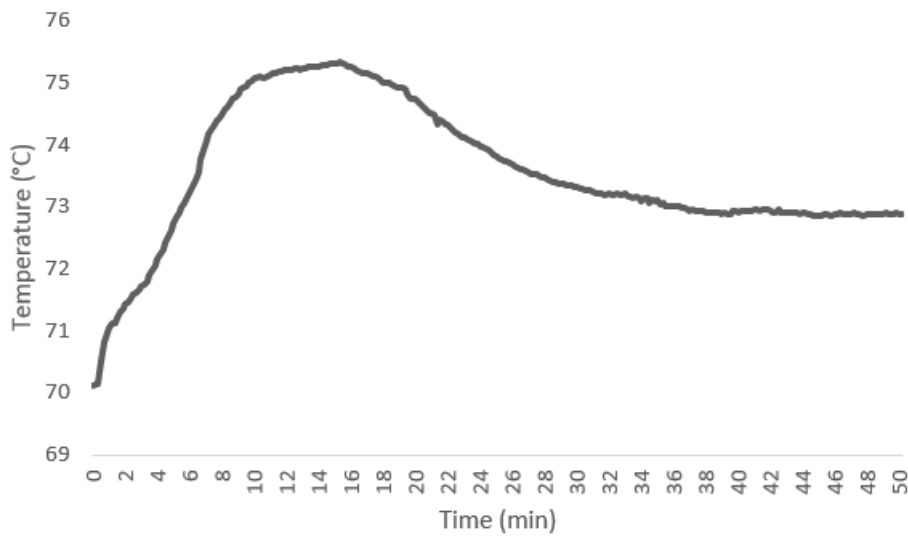


Figure 3.20: The XRG unit's geothermal fluid's inlet temperature measurements

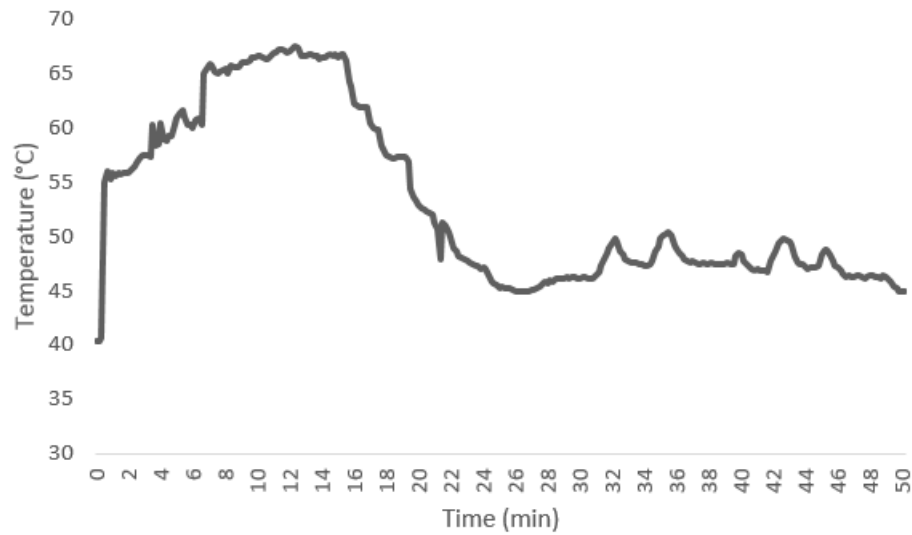


Figure 3.21: The XRG unit's geothermal fluid's outlet temperature measurements

The mass flow rate of the geothermal fluid was measurements are represented by Figure 3.22:

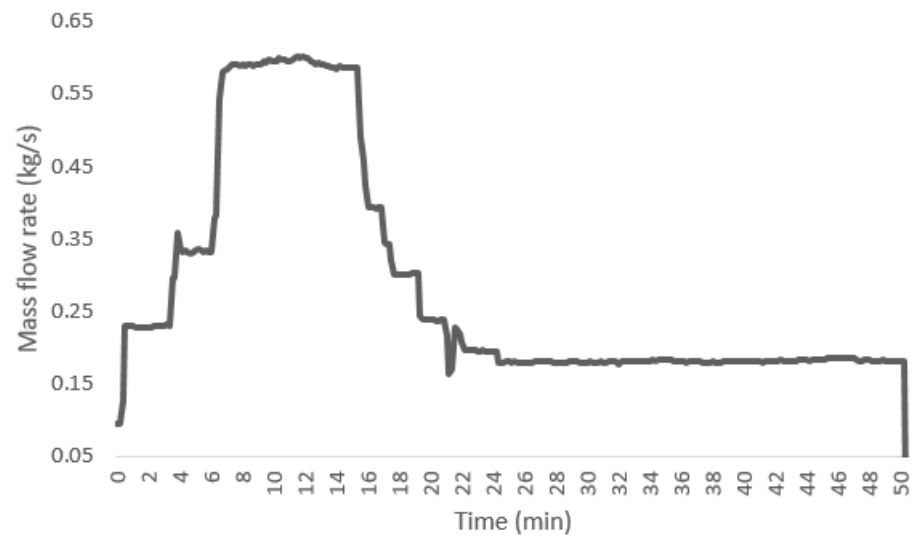


Figure 3.22: The XRG unit's mass flow rate of the hot water measurements

Measurements of the cooling waters temperature are seen on Figure 3.23 and the corresponding outlet temperatures on Figure 3.24

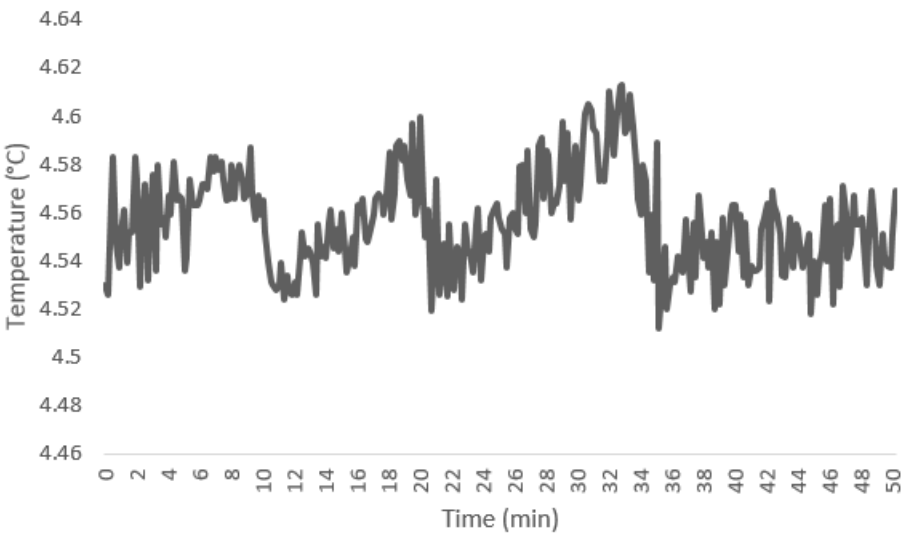


Figure 3.23: The XRG unit’s cooling water temperature inlet measurements

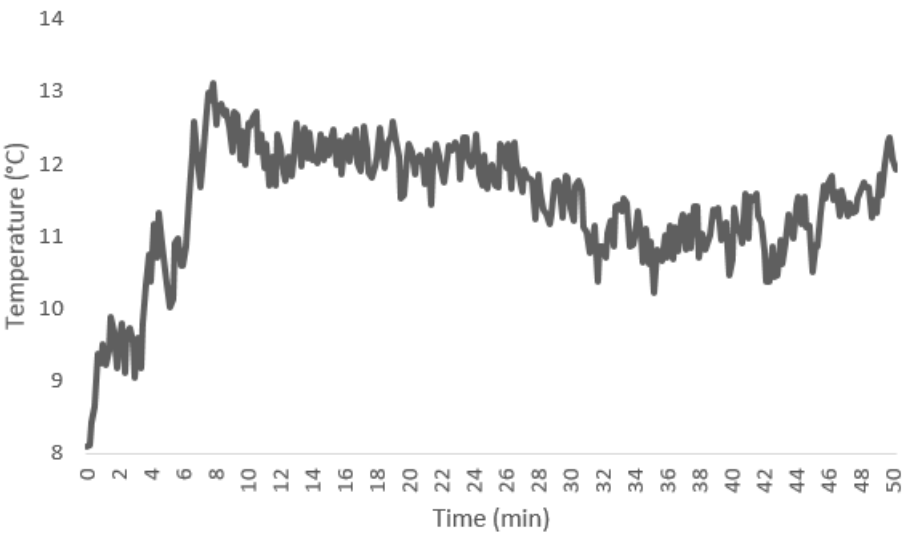


Figure 3.24: The XRG unit’s cooling water temperature outlet measurements

The mass flow rate of the cooling water is represented by Figure 3.25:

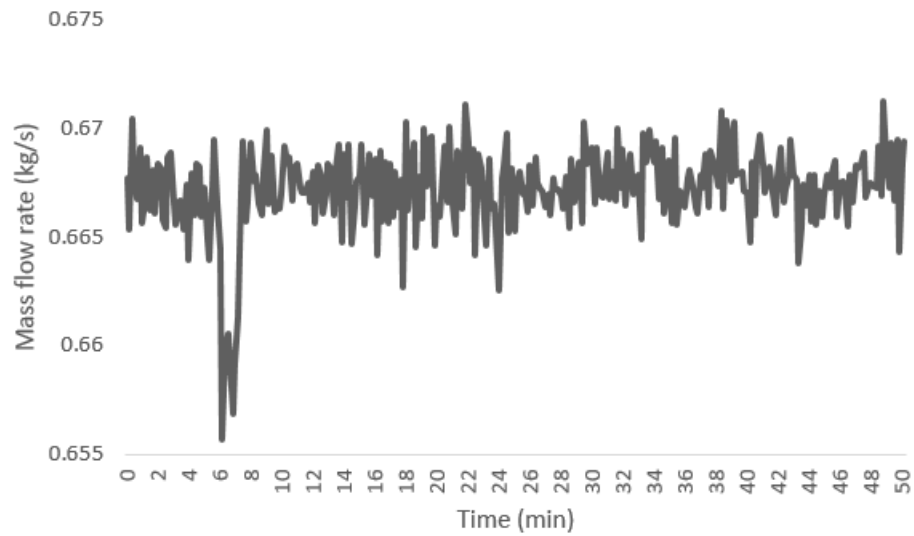


Figure 3.25: The XRG unit's mass flow rate of the cooling water measurements

Figure 3.26 shows the measured mass flow rate of the working fluid.

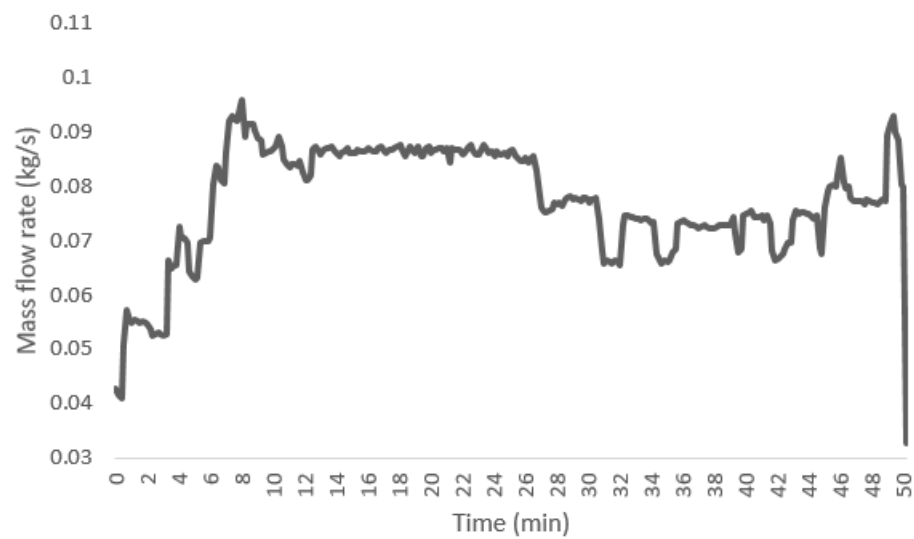


Figure 3.26: The XRG unit's mass flow rate of the working fluid measurements

The power output from the scroll expander was measured and is represented by Figure 3.27.

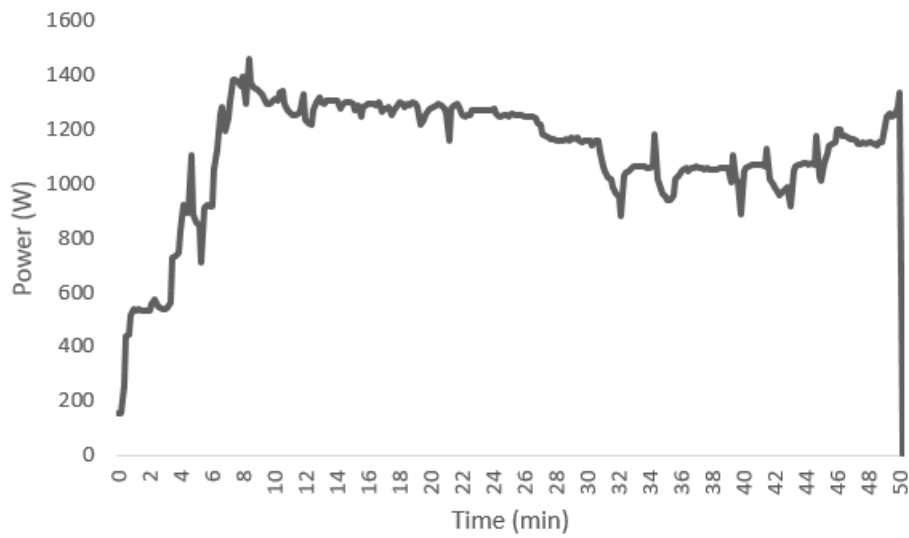


Figure 3.27: The XRG unit's scroll expander power output measurements

Figures 3.28 and 3.29 show temperature measurements for the inlet and outlet of the expander (states 4 and 5) and Figures 3.30 and 3.31 show the corresponding pressures.

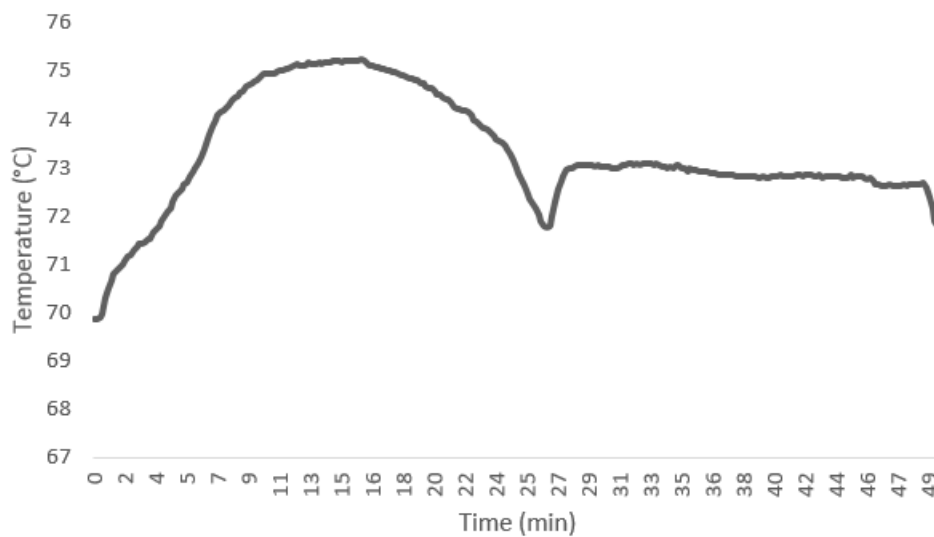


Figure 3.28: The XRG unit's scroll expander inlet temperature measurements

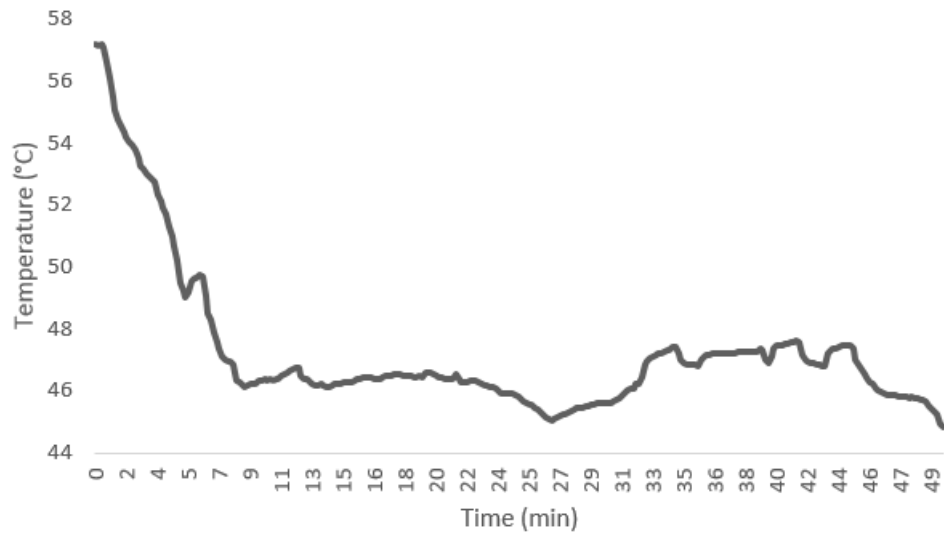


Figure 3.29: The XRG unit's scroll expander outlet temperature measurements

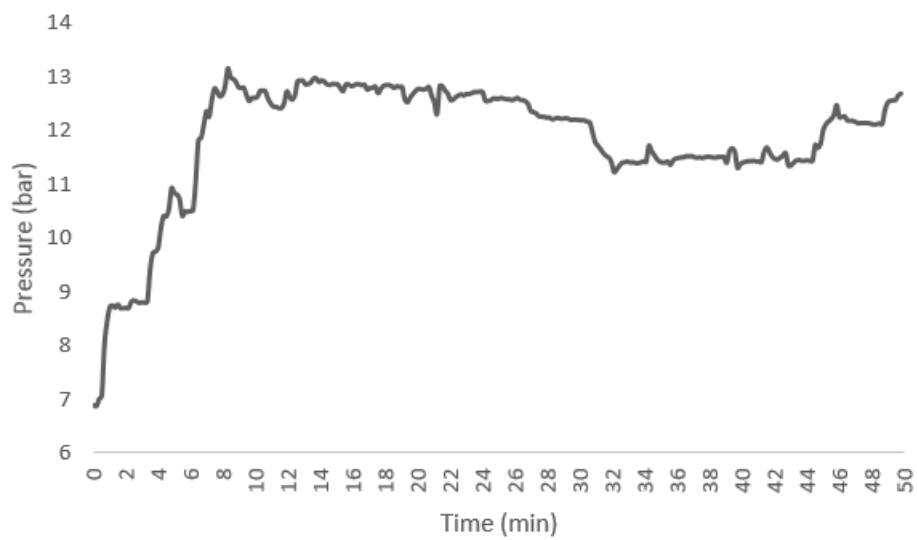


Figure 3.30: The XRG unit's scroll expander inlet pressure measurements

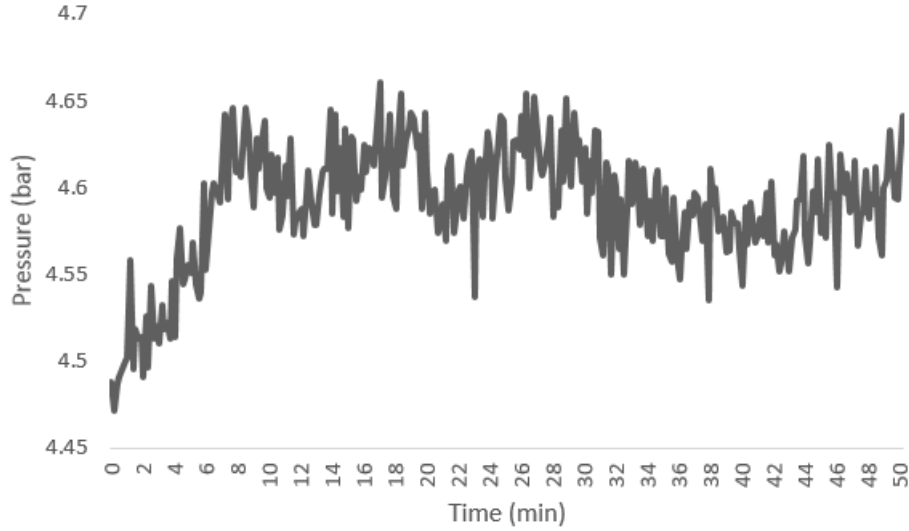


Figure 3.31: The XRG unit's scroll expander outlet pressure measurements

In order to properly compare the XRG's unit to this study's unit, the model must be altered. The main difference in calculations, is that the expander has a set volume ratio. This is the ratio of the specific volumes of the inlet and outlet of the expander. For the XRG unit's expander the ratio is set at 2,822 (Matthíasson, 2016). The ratio is then used to calculate the parameters at the outlet of the expander as well as the power output. This value is represented by Equation (3.27):

$$v_r = \frac{v_4}{v_5} \quad (3.27)$$

v_r is the volume ratio, v_4 is the specific volume at the expander's inlet and v_5 at the outlet.

Main parameters needed are listed in Table 3.9. The temperatures and the mass flow rate are average values from measurements, and the working fluid and volume ratio are constants. All other parameters remain the same.

Table 3.9: Parameters from the XRG unit

Parameter	Value
Working Fluid	R134a
\dot{m}_h [kg/s]	0,28
T_{hin} [°C]	73,55
T_{cin} [°C]	4,55
Volume Ratio	2,822

Chapter 4

Results

4.1 Base Case

The conditions chosen as the ideal case are summarized in Table 4.1. The table includes parameters calculated and estimated. These are the inputs best suited for a 100 kW net power output. Table 4.2 lists design parameters calculated and estimated for the heat exchangers. A graph showing how the most influential parameters effect the power output are seen on Figure 4.1. The graph shows how the temperature of the hot fluid inlet in the evaporator effects the mass flow rate of the working fluid for a net power output of 100 kW.

Table 4.1: Modelling results

Model parameters	
Working Fluid	R1234yf
\dot{m}_h [kg/s]	7,9
T_{hin} [°C]	100
T_{cin} [°C]	5
\dot{W}_{net} [kW]	100,5
η_{th} [%]	5,9
BWR	0,0823

Table 4.2: Heat exchangers design results

Heat exchangers	
Evaporator	
A_{boil} [m ²]	210,40
U_{boil} [kW/(m ² C)]	0,51
$\Delta T_{\text{lm,boil}}$ [°C]	16,67
Condenser	
A_{cond} [m ²]	182,24
U_{cond} [kW/(m ² C)]	0,65
$\Delta T_{\text{lm,cond}}$ [°C]	13,98

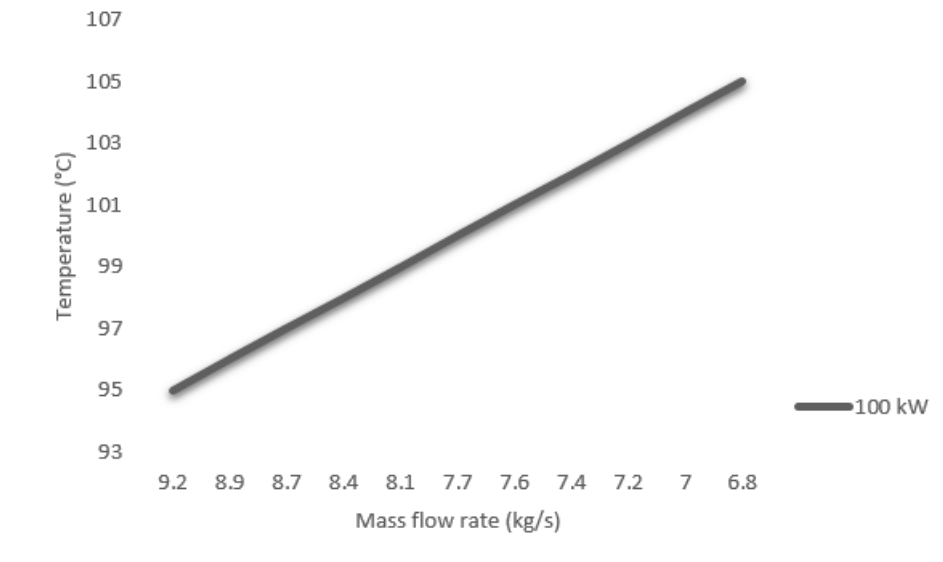


Figure 4.1: A visual representation of the effects of mass flow rate and temperature on net power output

4.2 Economic Feasibility Results

A summary of variables needed for the NPV calculations are in Table 4.4 as well as the total NPV calculated over 15 years. The NPV was calculated using Equation 3.23. The first ten years the costs are high since the greenhouse owner is paying the loan back. After that the only costs are the O&M costs. The benefits remain the same throughout the fifteen year period.

Table 4.3: Variables summary

Variable	Years	Amount [ISK]
Benefits	1-15	6.464.880
Costs	1-10	4.412.170
Costs	11-15	600.000
Cash flow	1-10	2.052.710
Cash flow	11-15	5.864.880
Discount rate		7,3%
Number of years		15
Net Present Value		23.738.602 ISK

4.3 Case Study Results

The case study's NPV calculation variables are summarized in Table 4.4. Benefits remain the same throughout the 15 year lifetime. Costs drop after the ten years it takes to pay up the loan. After ten years the only cost is the O&M costs. Cash flow is therefore negative in the first ten years.

A summary of the case study's model results for the greenhouse Friðheimar are listed in table 4.5. The table includes input parameters as well as results for the calculated power output.

Table 4.4: Case study NPV variables

Variable	Years	Amount [ISK]
Benefits	1-15	4.453.754
Costs	1-10	4.412.170
Costs	11-15	600.000
Cash flow	1-10	41.584
Cash flow	11-15	3.853.754
Discount rate		7,3%
Number of years		15
Net Present Value		6.986.438 ISK

Table 4.5: Case Study results

Friðheimar	
T_{hin} [°C]	94
\dot{m}_h [kg/s]	6
Direct lighting usage [%]	95
Total power needed [kWh/year]	6.000.000
\dot{W}_{net} [kW]	70,35
η_{th} [%]	6,25

4.4 Model Comparison

Average values from measurements taken in section 3.8 are listed in Table 4.6. These values were calculated based on the data discussed in section 3.8. State numbers refer to Figure 3.3. States locations can be seen in Figure 3.3 in subsection 3.3.1.

Table 4.6: Average values from measurements

Variable	
T_{hin} [°C]	73,55
T_{hout} [°C]	53,07
\dot{m}_h [kg/s]	0,28
T_{cin} [°C]	4,55
T_{cout} [°C]	11,45
\dot{m}_c [kg/s]	0,67
\dot{m}_{wf} [kg/s]	0,08
\dot{W}_{exp} [kW]	1,11
T_4 [°C]	73,3
T_5 [°C]	47,27
P_4 [bar]	11,85
P_5 [bar]	4,59

Some of the average values were compared with the outputs gotten from the model after alteration. These values are compared in Table 4.7.

Table 4.7: Comparison between the XRG unit and this studies unit

Variable	XRG unit	Altered model	Difference [%]
T_5 [°C]	47,27	45,38	4,16
\dot{W}_{exp} [kW]	1,11	1,11	0
\dot{m}_c [kg/s]	0,67	0,27	59,7
\dot{m}_{wf} [kg/s]	0,08	0,095	18,2
η_{th} [%]	4	5	25

Chapter 5

Discussion

In this chapter, the results from the previous chapter will be further analysed and discussed. Ideas for improvements and recommendations for future researched will be presented as well as a further analysis of limitations that affect the overall results of this study.

5.1 Base Case

The results of the base case are presented in Table 4.1. These parameters are the most influential to the power output of the unit. To deliver 100 kW of power the mass flow rate of the heat source needs to be 7,9 kg/s and the temperature 100 °C. Average values from the greenhouse owners result in a power output of 104,1 kW. It comes as no surprise that the most influential variables are the temperature and mass flow rate of the heat source. Figure 4.1 shows the relationship between those variables needed to produce 100 kW. It is the author's opinion that the temperature of 100 °C is the best choice for a net power output of 100 kW, as that is the average of the greenhouses researched, and the mass flow rate can be lower than the average value of 8,25 kg/s. Figure 4.1 is useful for different scenarios and a better understanding of influential parameters.

5.2 Working Fluid Selection

By looking at Table 3.4 it is apparent that fluids D4, D5, and Toluene have a higher boiling point than the low temperature geothermal resource at a given pressure. That means that in order for the working fluid to boil it has to be heated up to temperatures higher than the inlet temperature of the geothermal resource. Those fluids can, therefore, be disregarded.

Looking at the environmental properties, two working fluids in Table 3.5 stand out based on their values for the GWP factor. Those fluids are R134a and R245fa, both with factors over 1000, and on the higher end of atmospheric lifetime as well. Those fluids have been a popular choice in small scale ORC applications, but due to the increased environmental awareness in recent years, other options should be considered (Datla and Brasz, 2012). All of the other fluids measure in much lower values.

Comparing values in Table 3.6 two working fluids prove to be the safest choice, R1234yf and R1234ze(E) since they both have low toxicity and flammability. Out of those two R1234yf has a higher power output, at 104,1 kW even though it has lower efficiency. R1234yf is considered to be a good alternative to R134a (which is used in the XRG unit). According to a recent study, new regulations have been approved that states that only low GWP fluids will be permitted in HVACR (heating, ventilation, air conditioning and refrigeration) (Mota-Babiloni et al., 2015). The working fluid R1234yf is considered the best candidate for this model based on factors compared.

5.3 Economic Feasibility

The economic feasibility calculation results seen in Table 4.4, show the very high NPV value of almost 24 million ISK for the base case. This would indicate that the investment is extremely feasible for the greenhouse owner using this much electricity. Conservative assumptions were made regarding the greenhouse owner's lack of capital, but if the greenhouse owner were to get funding, the NPV would grow even further. Another interesting point to make is that the price of the unit could be lowered by various means. The price is based on similar units on the market, but the costs could be lowered if parts were built lo-

cally and by the use of scrap material. The XRG unit was built partially from scrap material and similar means could be taken for a larger unit (Gíslason, 2016). It is also safe to assume that this project could be funded by grants from various companies, or funds, interested in sustainable energy use or even the government. The mass flow rate is the total mass flow rate provided to the greenhouse. If the fluid were all to be used for the ORC unit the greenhouse could not heat up their facilities. The borehole used could possibly be stimulated to produce more, more provided to Friðheimar greenhouse or the fluid could be further used for heating after it exits the evaporator.

5.4 Case Study

The case study results indicate that the unit only produces 70,35 kW. This is considerably lower than the project's initial goal. This can be explained by the mass flow rate of the hot water. The mass flow rate is lower than the average of 8,25 kg/s, and therefore the power output is smaller. Even though the power output is low, the investment still has a positive NPV, as seen in Table 4.5. This concludes that the investment could be feasible for the owners of Friðheimar Greenhouse.

5.5 Model Comparison

After running the model with the XRG unit's parameters and average measured values, important factors were compared, as seen in Table 4.7. Most of the values are comparable within reason, but the highest difference is in the mass flow rate of the cooling water. This can be explained by different temperatures and pressures in different states in the cycle. Not all information on pressures and temperatures in other states was achieved, and therefore some unknown factors could be playing a determining role in the output values. However, the most important parameter, in the author's opinion, is the power output from the expander. The difference between those values is none.

Ideally these differences should be close to zero, but realistically there are bound to be some

variations. One of the smallest difference is in the temperature out of the expander. This is consistent with the volume ratio given. The volume ratio given is a deciding factor on the temperature out of the expander. In order to minimize other differences, more information would be needed on the thermodynamic properties at other states of the cycle.

The efficiency difference could also be explained by lack of data and could be further optimized given more comparable data. All that being said the average values from the measurements are likely to involve some degree of error. This is due to the earliest and latest values in the measurements, since they are, in some cases, vastly different from the average values calculated. In the author's opinion, these values don't have a deciding impact on the average values since they count for a very low percentage of the total data points.

5.6 Assumptions & Future Work

The limitations of this thesis include a number of factors.

The data collected from the greenhouse owners is considered fair, although future work might include a bigger poll for more accurate results. Future work could include accurate measurements, since the numbers acquired from the greenhouse owners rely largely on their memory and estimations.

Material selection relies heavily on the unknown chemistry of the geothermal resource in question, and therefore it was considered outside the scope of this thesis. Future work might include a comprehensive research on different materials to give a more accurate portrait of the model's outcome. This research would have to be site specific, since fluid's chemistry varies from one location to another. The material selected would have to withstand any corrosion and fouling from the fluid and should be selected according to both chemical and physical properties of the geothermal brine as well as the cooling water and the working fluid.

The comparison with the XRG unit is considered useful for the purpose of this study. Future work might include another model with all of the XRG's unit parameters. In order to correctly compare the two, the models would have to be run under the same conditions.

Regarding the feasibility calculations, the price for the unit is considered fairly accurate. It is also possible, with further research, that given more data from the greenhouse owners the price saved on electricity costs (the benefits) could shift somewhat, but it is considered minimal compared to the prices scale.

The biggest assumption made in this study is the mass flow rate present for the greenhouses, which is all being used in the ORC unit. This geothermal resource is currently being used for space heating, and the assumption is being made that there are more resources available for space heating purposes. Future work might include that the mass flow rate from the borehole could be increased by stimulation or other possible methods. Another possibility is that the fluid returned from the unit at 48,5°C could possibly be used for heating by mixing it with the fluid that is not needed for the ORC unit. This problem could be solved if the fluid returned from the evaporator is returned to the ground through a re-injection well. The mass flow rate of the well could then be increased substantially and enough fluid would be available both for heating and electricity production. According to the greenhouse owners, the current lighting systems lose a big amount of heat to the environment (the greenhouse) and if those bulbs were to be replaced with LED bulbs (that do not lose as much heat, but require less electricity), more water would be needed for space heating but less electricity would be needed. This would not be considered problematic, since the unit would require a lower mass flow rate and more could be used for heating. It would be interesting to find out how these changes would effect the unit.

5.7 Conclusion

The original goals strove to provide greenhouses with 100 kW of electrical power to assist them with artificial lighting. Greenhouses use a vast amount of electricity and the unit presented would aid in that task. In the author's opinion, this goal was met given some assumptions and limitations. After answering the why and how of this study's purpose, the author was curious to research if it would be beneficial for the greenhouse owner to invest in this unit. An economic feasibility analysis concluded, and the results show that this investment is well worth it for the greenhouse owner, even with conservative assumptions made

on his/her lack of private funding. In the author's opinion, the biggest influence would be the mass flow rate assumption. The flow from the borehole could be increased with various stimulation methods. The material and sizing limitations are in the author's opinion not as important, and are not expected to have a deciding effect on the pricing even though it would have delivered a more comprehensive result. The data from the greenhouses could be more substantial, but it serves its purpose of improving the author's understanding of how greenhouses utilize their resources. A more detailed comparison could be made with more data from the XRG unit, but this model is independent so it would not be necessary, but interesting.

Before this unit would be built it would be necessary to find out what mass flow rate is available for the unit, preferably with measurements taken at the site since greenhouse owners generally don't have exact numbers measured. Additionally, it would be interesting to find out if the fluid returned from the unit could be used in heating, possibly by mixing. An environmental study would also be preferred even though it is the author's believe that the unit would not cause problems due to the low toxicity of the fluid and the small size of the unit. More realistic case studies would be interesting for comparison, especially since this unit needs a mass flow rate higher than the average greenhouse has.

Bibliography

- Arshad, A. (2012). Net present value is better than internal rate of return. *Interdisciplinary Journal of Contemporary Research in Business*.
- Arvay, P., Muller, M. R., Ramdeen, V., & Cunningham, G. (2011). *Economic implementation of the organic rankine cycle in industry*. American Council for an Energy Efficient Economy.
- Ármannsson, K. R. (2016, August 21). *Private communications*. Friðheimar.
- Bergman, T. L., Lavine, A. S., Incropera, F. P., & DeWitt, D. P. (2011). *Fundamentals of heat and mass transfer*.
- Bjarnason, P. (2016, August 21). *Private communications*. Laugaland.
- Bombarda, P. (2016). *Estimating cost of the geothermal power technologies: main aspects and review*.
- Borunda, M., Jaramillo, O., Dorantes, R., & Reyes, A. (2015, August 20). Organic rankine cycle coupling with a parabolic trough solar power plant for cogeneration and industrial processes. *Renewable Energy*.
- Datla, B. V. & Brasz, J. (2012). *Organic rankine cycle system analysis for low gwp working fluids*. Purdue University.
- David, G., Michel, F., & Sanchez, L. (2011). Waste heat recovery projects using organic rankine cycle technology – examples of biogas engines and steel mills applications. In *World engineers convention*.
- Declaye, S., Quoilin, S., & Lemort, V. (2010, July 14). Design and experimental investigation of a small scale organic rankine cycle using a scroll expander. In *International refrigeration and air conditioning conference at perdue*.

- DiPippo, R. (2012). *Geothermal power plants: Principles, applications, case studies and environmental impact*.
- Electratherm. (2016). *6500 specification sheet*. Electrathem.
- Energy Technology Network. (2010, May). Geothermal heat and power. In *Energy technology systems analysis programme*.
- Enogia. (2016). *Enogia's eno-100lt orc system fact sheet*. Enogia.
- E-Rational. (2015, January). *E-rational orc-1000*. E-Rational.
- F-Chart Software. (2016). Engineering equation solver (ees). (Computer software). Madison, WI. Retrieved from <http://www.fchart.com/ees/>
- Friðheimar. (2016). Um friðheima. Retrieved from <http://fridheimar.is/is/um-fri%C3%B0heima>
- Georges, E., Declaye, S., Dumont, O., Quoilin, S., & Lemort, V. (2013, May 12). Design of a small scale organic rankine cycle engine used in a solar power plant.
- Gíslason, N. (2016). *Private communications*.
- Google Maps. (2016, December 27). Friðheimar farm. Retrieved from <https://www.google.com/maps/place/Fridheimar+Farm/@64.1764225,-20.4461051,673m/data=!3m1!1e3!4m5!3m4!1s0x48d696fbc383f7bb:0xdee6f1f7177295af!8m2!3d64.1789067!4d-20.4495008>
- Guðmundsson, B. (2016). *Private communications*. Orkustofnun.
- Harada, K. J. (2010, September 27). *Development of a small scale scroll expander* (Master's thesis, Oregon State University).
- Hettiarachci, M., Golubovic, M., Wore, W. H., & Ikegami, Y. (2006, April 17). *Optimum design criteria for an organic rankine cycle*. University of Illinois.
- IEA Geothermal. (2010). *Trends in geothermal applications. survey report on geothermal utilization and development in iea-gia member countries in 2010*. IEA Geothermal.
- Infinity Turbine. (2016). *Waste heat to power systems, organic rankine cycle*.
- Jakobsson, H. (2016, November 3). *Private communications*. Gufuhlíð.
- Jóhannesson, P. (2016). *Private communications*. Gróður.

- Lee, D. H., Yang, Y. M., Park, C. D., Lee, S. W., & Park, B. (2015, October 13). Development and test of a 100 kw class orc power-generator for low temperature geothermal applications.
- Lund, J. L. (2004). 100 years of geothermal power production. Research rep.
- Matthíasson, J. (2016, August 21). *Private communications*.
- Microgeneration. (2016). What is microgeneration? Retrieved from <http://www.microgeneration.com/professional-zone/Climate-Change/What-is-microgeneration>
- Mira Costa College. (2016). Plate tectonics. Retrieved from http://gotbooks.miracosta.edu/oceans/images/boundary_iceland.jpg
- Moran, M. J., Shapiro, H. N., Munson, B. R., & DeWitt, D. P. (2003). *Introduction to thermal systems engineering*. John Wiley & sons, Inc.
- Mota-Babiloni, A., Navarro-Esbrí, J., Molés, F., Cervera, Á. B., Peris, B., & Verdú, C. (2015, April 27). *A review of refrigerant r1234ze(e) recent investigations*. Institute for Industrial, Radiophysical and Environmental Safety (ISIRYM), Polytechnic University of Valencia, Camino de Vera s/n, E-46022 Valencia, Spain.
- Navea, J. G., Young, M. A., Xu, S., Grassian, V. H., & Stanier, C. O. (2011, February 16). The atmospheric lifetimes and concentrations of cyclic methylsiloxanes octamethylcyclotetrasiloxane (d4) and decamethylcyclopentasiloxane (d5) and the influence of heterogeneous uptake. *Atmospheric Environment*.
- Northern Lights. Solar Solutions. (2016). Solar plate heat exchanger. Retrieved from <https://www.solartubs.com/solar-plate-heat-exchanger.html>
- Nouman, J. (2012, September 17). *Comparative studies and analyses of working fluids for organic rankine cycles - orc* (Master's thesis, KTH School of Industrial Engineering and Management).
- Nýsköpunarmiðstöð Íslands. (2015, September 13). Bylting í vinnslu rafmagns úr jarðvarma. Retrieved from <http://www.nmi.is/frettir/2015/09/bylting-i-vinnslu-rafmagns-ur-jardvarma/>
- Ocko, I. (2016). What sparked global warming? people did. *Environmental Defence Fund*.
- Orkusetur. (2016). *Samanburður á raforkuverði til heimila*. Orkusetur.

- Orkustofnun. (2016). Orkuvefsjá. Retrieved from <http://www.orkuvefsja.is/vefsja/orkuvefsja.html>
- Ólafsson, P. (2016, August 21). *Private communications*. Hveravellir.
- Quoilin, S. (2008, November). *An introduction to thermodynamics applied to organic rankine cycles*. University of Liège.
- Quoilin, S., Declaye, S., Legros, A., Guillaume, L., & Lemort, V. (2012). *Working fluid selection and operating maps for organic rankine cycle expansion*. University of Liège.
- Scilab Enterprises. (2015). Scilab. (Computer software).
- Seðlabanki Íslands. (2016). *Ársskýrsla 2015*. Seðlabanki Íslands.
- Seta, A. L., Andreasen, J. G., Pierobon, L., Persico, G., & Hagaling, F. (2015, October 13). Design of organic rankine cycle power systems accounting for expander performance.
- Stefánsson, L. D. (2016, August 21). *Private communications*. Reykjaflöt.
- Sævarsson, Ó. (2016, December 2). *Private communications*. Heiðmörk.
- Tang, Y. (2014, July 15). Combined rankin and organic rankine cycles with screw expanders.
- Tewari, K., Agrawal, S., & Arya, R. K. (2014, December 12). Generalized pinch analysis scheme using matlab.
- Thulukkanam, K. (2013). *Heat exchanger desing handbook. second edition*. CRC Press. Taylor & Francis Group.
- Vilhjálmsón, J., Baldursson, I., & Hallgrímsson, J. H. (2015). *Raforkuspá 2015*. Orkustofnun.
- Waldorff, M. (2016, November 11). *Private communications*.
- Wei, D., Lu, X., Lu, Z., & Gu, J. (2006). Performance analysis and optimization of organic rankine cycle (orc) for waste heat recovery.
- Weiß, A. P. (2015, October 13). Volumetric expander versus turbine- which is the better choice for small orc plants. University of Applied Sciences. Amberg, Germany.
- Zuccato Energia. (2016). *Product sheet. 100 kw, skid mounted, low temperature organic rankine cycle (lt-orc) energy production module*. Zuccato Energia.
- Porgeirsson, G. (2016, October 31). *Private communications*. Ártangi.

Appendix A

Code

Modelling performed in Engineering Equation Solver (EES)

Symbol	Description	Unit
m_dot	Mass flow rate	[kg/s]
T	Temperature	[C]
P	Pressure	[bar]
h	Enthalpy	[kJ/kg]
in	Inlet	
out	Outlet	
h	Geothermal fluid	
c	Cooling water	
cp	Specific heat	[kJ/kgC]
rho	Density	[kg/m ³]
mu	Viscosity	[kg/ms]
1,2,3,4,5,6,7,8	Cycle states	
is	Isentropic	
pinch	Pinch point temperature	[C]
boil	Evaporator	
cond	Condenser	
X	Steam quality	
s	Entropy	[kJ/C]
eta	Efficiency	
BWR	Back work ratio	
Q	Heat transfer rate	[kW]
W	Power	[kW]
delta	Difference	

Working fluid

Fluid\$='R1234yf'

Geothermal fluid for evaporator

$$\dot{m}_h = 8.25$$

$$T_{hin} = 100.23$$

$$P_{hin} = 3$$

$$\text{pinch}_{boil} = 5$$

$$\dot{m}_h(h_{hin} - h_{h2}) = (\dot{m}_{wf}(h[4] - h[2]))$$

$$\dot{m}_h = (\dot{m}_{wf}(h[4] - h[1])) / (h_{hin} - h_{hout})$$

$$h_{hin} = \text{Enthalpy}(\text{Water}, T = T_{hin}, P = P_{hin})$$

$$c_{p,hin} = \text{Cp}(\text{Water}, h = h_{hin}, P = P_{hin})$$

$$P_{hout} = P_{hin}$$

$$T_{hout} = \text{Temperature}(\text{water}, P = P_{hout}, h = h_{hout})$$

$$c_{p,hout} = \text{Cp}(\text{Water}, h = h_{hout}, P = P_{hout})$$

$$\rho = \text{Density}(\text{water}, T = T_{hin}, h = h_{hin})$$

$$T_{h2} = T[2] + \text{pinch}_{boil}$$

$$h_{h2} = \text{Enthalpy}(\text{water}, T = T_{h2}, P = P_{hin})$$

$$\dot{m}_h(h_{h3} - h_{h2}) = \dot{m}_{wf}(h[3] - h[2])$$

$$T_{h3} = \text{Temperature}(\text{water}, h = h_{h3}, P = P_{hin})$$

Cooling water for condenser

$$T_{cin} = 5$$

$$P_{cin} = 1$$

$$\text{pinch}_{cond} = 5$$

$$m_dot_c = (m_dot_wf*(h[5]-h[8]))/(h_cout-h_cin)$$

$$m_dot_c = (m_dot_wf*(h[6]-h[8]))/(h_c_6-h_cin)$$

$$h_cin = \text{Enthalpy}(\text{Water}, T = T_cin, P = P_cin)$$

$$cp_cin = \text{Cp}(\text{Water}, h = h_cin, T = T_cin)$$

$$P_cout = P_cin$$

$$T_cout = \text{Temperature}(\text{water}, h = h_cout, P = P_cout)$$

$$cp_cout = \text{Cp}(\text{Water}, h = h_cout, T = T_cout)$$

$$T_c_6 = T[6] - \text{pinch_cond}$$

$$h_c_6 = \text{Enthalpy}(\text{water}, T = T_c_6, P = P_cin)$$

$$m_dot_c*(h_c_6-h_c_7) = m_dot_wf*(h[6]-h[7])$$

$$T_c_7 = \text{Temperature}(\text{water}, h = h_c_7, P = P_cin)$$

Pump-Preheater

$$P[1] = P[4]$$

$$T[1] = \text{Temperature}(\text{Fluid}\$, P = P[1], h = h[1])$$

$$s[1] = s[8]$$

$$h_1_is = \text{Enthalpy}(\text{Fluid}\$, s = s[1], P = P[1])$$

$$cp[1] = \text{Cp}(\text{Fluid}\$, T = T[1], P = P[1])$$

Preheater-Evaporator

$$X[2] = 0$$

$$P[2] = \text{Pressure}(\text{Fluid}\$, T = T[2], X = X[2])$$

$$h[2] = \text{Enthalpy}(\text{Fluid}\$, T = T[2], X = X[2])$$

$$s[2] = \text{Entropy}(\text{Fluid}\$, X = X[2], h = h[2])$$

$$cp[2] = \text{Cp}(\text{Fluid}\$, h = h[2], P = P[2])$$

Evaporator-Superheater

$$T[3] = T[2]$$

$$X[3] = 1$$

$$P[3] = P[2]$$

$$s[3] = \text{Entropy}(\text{Fluid}\$, X = X[3], P = P[3])$$

$$cp[3] = \text{Cp}(\text{Fluid}\$, s = s[3], P = P[3])$$

$$h[3] = \text{Enthalpy}(\text{Fluid}\$, T = T[3], X = X[3])$$

Superheater-Turbine

$$\text{superheat} = 10$$

$$T[4] = T[3] + \text{superheat}$$

$$P[4] = P[3]$$

$$h[4] = \text{Enthalpy}(\text{Fluid}\$, T = T[4], P = P[4])$$

$$s[4] = \text{Entropy}(\text{Fluid}\$, T = T[4], P = P[4])$$

$$cp[4] = \text{Cp}(\text{Fluid}\$, T = T[4], P = P[4])$$

$$v[4] = \text{Volume}(\text{Fluid}\$, T = T[4], P = P[4])$$

Turbine-De Superheater

$$T[5] = \text{Temperature}(\text{Fluid}\$, P = P[5], h = h[5])$$

$$s[5] = \text{Entropy}(\text{Fluid}\$, P = P[5], h = h[5])$$

$$cp[5] = \text{Cp}(\text{Fluid}\$, T = T[5], P = P[5])$$

$h_{5_is} = \text{Enthalpy}(\text{Fluid}\$, s = s[4], P = P[5])$

$v[5] = \text{Volume}(\text{Fluid}\$, T = T[5], P = P[5])$

De Superheater-Condenser

$X[6] = 1$

$P[6] = P[5]$

$P[6] = \text{pressure}(\text{Fluid}\$, T = T[6], x = 0)$

$h[6] = \text{Enthalpy}(\text{Fluid}\$, T = T[6], X = X[6])$

$s[6] = \text{Entropy}(\text{Fluid}\$, X = X[6], P = P[6])$

Condenser-Sub Cooler

$P[7] = P[6]$

$T[7] = T[6]$

$X[7] = 0$

$h[7] = \text{Enthalpy}(\text{Fluid}\$, T = T[7], x = x[7])$

$s[7] = \text{Entropy}(\text{Fluid}\$, X = X[7], P = P[7])$

$cp[7] = \text{Cp}(\text{Fluid}\$, h = h[7], P = P[7])$

Sub Cooler-Pump

$P[8] = P[5]$

$T[8] = T[7] - \text{subcooling}$

$X[8] = 0$

$h[8] = \text{Enthalpy}(\text{Fluid}\$, T = T[8], P = P[8])$

$s[8] = \text{Entropy}(\text{Fluid}\$, T = T[8], P = P[8])$

$$v[8] = \text{Volume}(\text{Fluid}\$, T = T[8], P = P[8])$$

$$cp[8] = \text{Cp}(\text{Fluid}\$, T = T[8], P = P[8])$$

Efficiencies & Power

$$\eta_{\text{turb}} = 0.8$$

$$\eta_{\text{turb}} = (h[4] - h[5]) / (h[4] - h_{5,\text{is}})$$

$$\eta_{\text{th}} = (W_{\text{dot_net}} / Q_{\text{dot_boil}})$$

$$\eta_{\text{car}} = 1 - (T[5] + 273.15) / (T[4] + 273.15)$$

$$\eta_{\text{pump}} = 0.8$$

$$\eta_{\text{pump}} = (h_{1,\text{is}} - h[8]) / (h[1] - h[8])$$

$$\text{BWR} = W_{\text{dot_pump}} / W_{\text{dot_turb}}$$

$$W_{\text{dot_turb}} = (m_{\text{dot_wf}} * (h[4] - h[5])) * \eta_{\text{turb}}$$

$$W_{\text{dot_pump}} = v[8] * m_{\text{dot_wf}} * (P[1] - P[8]) * 100 / \eta_{\text{pump}}$$

$$W_{\text{dot_net}} = (W_{\text{dot_turb}} - W_{\text{dot_pump}})$$

Heat exchangers heat transfer rate

$$Q_{\text{dot_boil}} = (m_{\text{dot_wf}} * (h[4] - h[1]))$$

$$Q_{\text{dot_cond}} = (m_{\text{dot_wf}} * (h[5] - h[8]))$$

$$Q_{\text{dot_PH}} = m_{\text{dot_wf}} * (h[2] - h[1])$$

$$Q_{\text{dot_EV}} = m_{\text{dot_wf}} * (h[3] - h[2])$$

$$Q_{\text{dot_SH}} = m_{\text{dot_wf}} * (h[4] - h[3])$$

$$Q_{\text{dot_DSH}} = m_{\text{dot_wf}} * (h[5] - h[6])$$

$$Q_{\text{dot_C}} = m_{\text{dot_wf}} * (h[6] - h[7])$$

$$Q_dot_SC = m_dot_wf*(h[7]-h[8])$$

LMTD

$$\Delta T_1 = T_{hin} - T[4]$$

$$\Delta T_2 = T_{hout} - T[1]$$

$$\Delta T_3 = T[8] - T_{cin}$$

$$\Delta T_4 = T[5] - T_{cout}$$

$$\Delta T_{lm_boil} = ((\Delta T_2) - (\Delta T_1)) / ((\ln(\Delta T_2 / \Delta T_1)))$$

$$\Delta T_{lm_cond} = ((\Delta T_4) - (\Delta T_3)) / ((\ln(\Delta T_4 / \Delta T_3)))$$

$$SS[4] = \text{SoundSpeed}(\text{fluid}, T = T[4], P = P[4])$$

$$SS[5] = \text{SoundSpeed}(\text{fluid}, T = T[5], P = P[5])$$



School of Science and Engineering
Reykjavík University
Menntavegur 1
101 Reykjavík, Iceland
Tel. +354 599 6200
Fax +354 599 6201
www.ru.is